Photofission at sub-barrier excitations

Yu. B. Ostapenko, G. N. Smirenkin, and A. S. Soldatov

Physics and Power Institute, Obninsk

Yu. M. Tsipenyuk

Institute of Physics Problems, Moscow

Fiz. Elem. Chastits At. Yadra **12**, 1364–1431 (November–December 1981)

The review is devoted to investigations of the probability of photofission in the threshold region and in the sub-barrier region of energies. The following questions of the physics of low-energy fission are the main subjects of interest: the spectrum of transition states (fission channels) of cold nuclei, the shape of the barrier, the symmetry of the nuclear configuration in the process of deformation, the features of the passage through the barrier associated with the existence in the second well of the quasistationary fission and nonfission modes, and the interaction between them and between them and the analogous states in the first well. The nature of this interaction depends strongly on the energy, which explains the increasing interest in a new field of investigation: deep sub-barrier fission near the bottom of the second well, in particular, the isomer shelf effect observed at such energies. The present state of work in this direction is analyzed critically.

PACS numbers: 25.85.Jg, 27.90. + b

INTRODUCTION

The structure of the potential-energy surface of a nucleus has a decisive influence on the behavior of a fissioning system in the region of the potential barrier which arises during the process of deformation of the nucleus and, above all, on the most important characteristic—the fission probability. For a long time, ideas about the shape of the fission barrier were based on the liquid-drop model, which gave a smooth single-hump curve for the dependence of the nuclear potential energy on the main deformation coordinate leading to fission.

In 1966–1967, Strutinskiĭ[1,2] developed the shell-correction method, and its application to fissioning systems showed that during the fission process the deformation energy of the nucleus oscillates about the smooth dependence described by the liquid-drop model. For the actinides, this fundamental fact leads to the prediction of a two-hump shape of the barrier with humps of nearly equal height. The new ideas about the fission process of heavy nuclei became known as the two-hump barrier model.[3-5]

The more accurate knowledge of the barrier shape had a significant influence on the physics of the fission process and led to a significant modification of ideas which had changed little during the almost 30 years which had passed since the pioneering studies of Bohr, Wheeler, and Frenkel'.[6,7] The presence in the new model of two saddle points with their spectra of transition states and the fairly deep minimum between them, in which a system of quasistationary levels that interact with the levels of the first well (Fig. 1) can be formed, complicated but at the same time greatly enriched the picture of fission with interesting physical consequences. The development of the new ideas (see Refs. 3–5 and 8–10) made it possible to understand the nature of some phenomena which had baffled the previous theory, for example, spontaneously fissioning isomers, various types of resonance structure in the cross sections of sub-barrier fission, anomalies in the dependence of the fission thresholds and the anisotropy of the angular distribution of the fragments on the nucleon composition of the nucleus, and so forth. In addition, the new ideas stimulated the development of experimental investigations of the fission process and the properties of anomalously deformed nuclear states.

The greatly increased interest of physicists in the investigation of deep sub-barrier fission is appropriate. The probability of fission of heavy nuclei is determined by the interaction between the systems of levels of the first and second well and by the interaction of the fission and nonfission states within each system, which significantly change their nature as one moves into the sub-barrier region of energies on account of both the exponential decrease in the penetrability of the barrier humps and the exponential growth of the distances between the levels. The interest in this new situation in fission physics is stimulating experiments aimed in the first place at studying the fission cross section and the angular distribution of the fragments in the widest possible range of sub-barrier energies.

The searches for a suitable method of excitation to solve this problem lead to the photofission reaction, since the use of γ rays does not involve the fundamental restrictions on the energy inherent in fission reac-

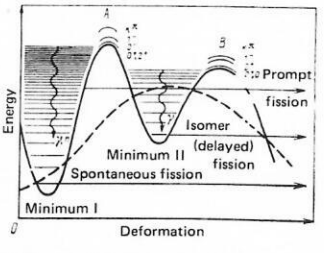

FIG. 1. Schematic representation of the fission barrier in the two-hump model. The inner hump is A, the outer one B. The result of calculation in the liquid-drop model is also shown (broken curve). The sections of curves near the tops of the humps show the possible positions of the fission channels (for an even-even nucleus).

 0090-4759/81/060545-29$02.80

tions induced by neutrons or charged particles, and the use of high-current electron accelerators to produce bremsstrahlung of high intensity significantly extends the limits to the experimental possibilities set by the decrease in the number of detectable induced-fission events in the deep sub-barrier region. In addition, photoabsorption is characterized by a uniquely simple spectrum of angular momenta transferred to the nucleus, and this is of fundamental importance in the investigation of quantum effects in fission, the description and interpretation of which are greatly complicated in the two-hump model. Let us consider this in more detail.

At energies near the fission threshold (around 6 MeV), the photon wavelength $\lambda\!\!\!^{-}$ is significantly greater than the radius R of the nucleus, namely,

$$R/\lambda\!\!\!^{-} \approx 1/5, \tag{1}$$

so that the contribution of photons with different multipolarity to the total interaction cross section σ_γ decreases rapidly with increasing angular momentum l:

$$\sigma_\gamma^{El}/\sigma_\gamma^{E1} \approx (R/\lambda\!\!\!^{-})^{2l}; \quad \sigma_\gamma^{Ml}/\sigma_\gamma^{E1} \approx (R/\lambda\!\!\!^{-})^{2(l+1)}. \tag{2}$$

The predominance of the electric dipole interaction E1 can be characterized by an estimate which follows from (1) and (2) for the ratio of the cross sections σ_γ for the lowest multipolarities:

$$\sigma_\gamma^{E2}/\sigma_\gamma^{E1} \approx \sigma_\gamma^{M1}/\sigma_\gamma^{E1} \approx (R/\lambda\!\!\!^{-})^2 \approx 1/25, \tag{3}$$

from which it follows that γ rays with multipolarities higher than E2 and M1 can be ignored. Figure 2 shows the distribution $\varphi(l)$ of the angular momenta transferred to the nucleus in the reactions most widely used to study the threshold and sub-barrier effects in the fission of heavy nuclei. The simplicity of the spectrum $\varphi(l)$ is undoubtedly the main advantage of the (γ, f) reaction, giving it a distinguished place in fission physics.

By means of the (γ, f) reaction some fundamental results, including the discovery of angular anisotropy of fission,[11] were already obtained in the fifties, but the systematic investigation of low-energy photofission became possible later with the appearance of track detectors,[12] which completely solved the problem of suppressing the γ-ray background in fragment detection, and the development of sources such as the high-current microtron,[13,14] which ensured electron beams with high intensity and energy resolution. Experiments were begun in 1964 at the Institute of Physics Problems using the microtron with 17 orbits, and they were continued for 15 years in collaboration with the Physics and Power Institute. The majority of data so far accumulated on threshold and especially sub-barrier photofission of heavy nuclei were obtained in these experiments. The present review is based mainly on this experimental information.

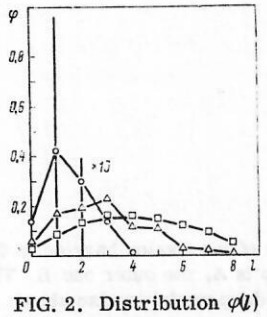

FIG. 2. Distribution $\varphi(l)$ of the orbital angular momenta transferred to the nucleus in the following reactions: (γ, f), the vertical lines ($E_\gamma = 5-7$ MeV); (n, f), the circles ($E_n = 1$ MeV); (d, pf), the triangles ($E_d = 15$ MeV); and (t, pf), the squares ($E_t = 18$ MeV).

Three main questions are discussed.

1. The investigations of photofission in the region of the threshold, aimed at the verification and experimental justification of the ideas about the spectrum of fission channels that follow from the hypothesis of A. Bohr and the two-hump model.

2. The experimental investigations of deep sub-barrier photofission and the isomer-shelf effect which occurs in this region.

3. The interpretation of sub-barrier photofission effects. The channel analysis of the experimental data in the framework of the description of the fission probability which uses the concept of doorway states.

1. ANGULAR ANISOTROPY OF PHOTOFISSION AND STRUCTURE OF THE BARRIER

Experimental verification of A. Bohr's hypothesis. The discovery in 1952 by Winhold, Demos, and Halpern[11] of angular anisotropy of the fragments in the ^{232}Th(γ, f) reaction was the point of departure in the development of quantum aspects in the ideas about the mechanism of the fission process, which had been constructed earlier on the basis of the classical concepts of the quasimolecular model and the liquid-drop model. The experiment[11] showed that the fission fragments from the photofission of ^{232}Th are emitted preferentially at a right angle to the direction of the γ-ray bremsstrahlung beam, following the distribution

$$W(\vartheta) = a + b \sin^2 \vartheta, \tag{4}$$

in which the ratio

$$b/a = W(90^\circ)/W(0^\circ) - 1, \tag{5}$$

which characterizes the angular anisotropy, decreases with increasing limiting energy E_{max} of the spectrum. This property was discovered in all the investigated even–even nuclei from ^{226}Ra to ^{242}Pu.[15-23]

To explain the anisotropy of the angular distribution of the fragments, A. Bohr[24] put forward in 1955 the idea of fission channels, specific quantum states of the fissioning nucleus at the saddle point, and the suggestion that their spectrum is similar to the excitation spectrum of a nucleus with equilibrium deformation. It is important that these are states of nuclei with anomalous deformation and even more that they correspond, not to a minimum of the potential energy like the levels of ordinary nuclei, but to a maximum—an extremely unstable state in the fission process. Further, in accordance with Bohr's hypothesis each fission channel has its own deformation potential-energy surface deter-

mined by a set of quantum numbers, namely, J, the angular momentum of the nucleus, K, its projection onto the direction of fission, which coincides with the symmetry axis (as in the equilibrium state, the nucleus is assumed to have axial symmetry), and π, the parity of the state. It is assumed that K can be a fairly "good" approximate quantum number as the fissioning nucleus descends from the saddle point to the scission point. The resulting dependence of the barrier height on the quantum numbers $\lambda = (J, \pi, K)$ ensures an inhomogeneous K distribution, and in the presence of a definite alignment of the angular momenta J of the compound nucleus in space this leads to an angular anisotropy in the emission of the fragments relative to the direction of the incident beam. The angular distribution of the fragments in the case of fission through a channel with fixed quantum numbers J and K is described by the relation

$$W_{JK}(\vartheta) = \frac{2J+1}{8}\{|D^J_{M,K}(\vartheta)|^2 + D^J_{-M,K}(\vartheta)|^2\}, \quad (6)$$

where $D^J_{M,K}(\vartheta)$ is a Wigner function, and M is the projection of J onto the direction of the beam. The angular distribution (4) of the fragments observed in the (γ, f) reaction corresponds to the theoretically expected distribution in the case of an E1 interaction with an even–even nucleus, for which

$$J = l = 1;\ M = \pm 1;\ K = 0 \text{ and } 1,$$

as can be readily seen by examining the angular dependences of the Wigner functions:

$$W_{10}(\vartheta) \sim |D^1_{\pm 1,0}(\vartheta)|^2 \sim \sin^2\vartheta;\ |W_{1,1}(\vartheta) \sim |D^1_{\pm 1,1}(\vartheta)|^2 \sim 1 - (1/2)\sin^2\vartheta. \quad (7)$$

Assuming that the fission barriers have different heights for the channels $J^\pi = 1^-$, $K = 0$ and 1, Bohr explained not only the origin of the angular anisotropy of fission but also its energy dependence.

The fruitfulness of Bohr's hypothesis of fission channels was soon recognized and widely used to interpret various data on fission near the threshold. The modern description of the fission probability is based on the hypothesis. At the same time, there is a difficulty of interpretation inherent in the concepts of fission channels, and this was given expression, for example, in Ref. 25: "The assumed 'spectrum' at the barrier is at best quasistationary, and, in fact, the notion of such a spectrum is an accurate one only if the nucleus remains at the barrier for a time long compared with the periods of the excitations in question." The question of the fulfillment of the condition of quasistationarity of the spectrum of transition states, which is intimately related to more general questions such as the space-time picture of fission, the dynamics of the process, and the viscosity of nuclear matter, cannot be solved in a theoretical framework (there is still no satisfactory answer to it). Therefore, the adequacy of the ideas about the spectrum of fission channels can be established only experimentally.

Besides the interpretation based on the hypothesis of fission channels, the possibility was noted[26] of a model-free description of the main properties of the anisotropy in the fragment angular distribution in which the K distribution is specified at the time of formation of the fragments and not at the top of the barrier. A way of choosing between the two possibilities and simultaneously testing Bohr's hypothesis consists of establishing experimentally unambiguously interpretable properties of the angular anisotropy that cannot occur in the alternative (fragment) description. It is obvious that these properties, which reflect the discreteness of the spectrum of fission channels, must be most clearly manifested in the region of the fission threshold. In the alternative description, the region of the threshold is in no way distinguished.

Definite predictions follow from Bohr's hypothesis only for the fission-channel spectrum of even–even nuclei, for which the pairing of the nucleons ensures that the quantum numbers of the ground state, $K^\pi = 0^+$, and the energy gap in the spectrum of internal excitations are conserved during the deformation process. Concerning the spectrum of the collective excitations within the energy gap, Bohr[24] said the following: "For nuclei, whose shape possesses reflection symmetry, the channel spectrum contains, for $K = 0$, only the rotational levels with even J-values: $0, 2, 4, \ldots$, which all have positive parity. The observed mass ratio of the fission fragments indicates, however, that at the saddle point the nuclear shape in general does not possess reflection symmetry. The rotational band then also contains the odd J-values, having negative parity; however, the negative parity levels will be displaced with respect to the positive parity levels by an amount $\hbar\omega_{\text{inv}}$, where ω_{inv} is the frequency of the tunneling motion between the mirror shapes of the preferred symmetry. The more pronounced the asymmetry is, the smaller will be the ω_{inv}." And further: "At the saddle point shape one thus expects even–even nuclei to have a lowest state of $J^\pi = 0^+$, and close lying collective excitations of $2^+, 4^+, \ldots$ type as, although with somewhat higher energies, states of $1^-, 3^-, \ldots$ type." Levels with $K \neq 0$, which are situated higher, correspond to more complicated types of excitation.

A small number of channels participating in fission and a sufficient distance between them is another important requirement needed for the subject of investigation. It is advanced in connection with the finite tunneling barrier penetrability

$$T(E, E_f^\lambda) = \{1 + \exp[(2\pi/\hbar\omega_\lambda)(E - E_f^\lambda)]\}^{-1} \quad (8)$$

for $E < E_f^\lambda$, which smoothes the individual effects of the individual fission channels if the distance between them is $E_f^{\lambda'} - E_f^\lambda \lesssim \hbar\omega/2\pi \approx 0.1$–$0.2$ MeV, where $\hbar\omega_\lambda = \hbar\omega$ is the curvature parameter of the barrier, which here and in what follows is (for the sake of simplicity and in connection with the smallness of $E_f^{\lambda'} - E_f^\lambda$ compared with the height of the barrier) taken to be the same for all the considered λ.

In this sense, even–even nuclei are the best if not the only significant source of information about phenomena relating to the discrete structure of the fission-channel spectrum. But not only the choice of the type of fissioning nuclei but also the method of their excitation is important. The lack of ambiguity in the interpretation of the experimental data depends decisively on the

extent to which the set of admissible states is restricted with respect to the spin and parity in the doorway channel of the reaction.

From the adopted point of view, photofission of even–even nuclei offers a unique possibility for direct verification of Bohr's hypothesis. If the energy of the γ rays is near the threshold, just two channels, $J^\pi = 2^+$ and 1^-, $K = 0$, which are excited by electric quadrupole (E2) and dipole (E1) absorption, will play dominant roles in the fission. These are the first excited states, and, significantly, they belong to the lowest rotational bands of the fission channels predicted by Bohr. The partial contribution of each of them can be reliably established experimentally from the shape of the angular distribution $W(\vartheta)$; namely, the quadrupole component

$$W_{20}(\vartheta) \sim |D^2_{\pm 1,0}(\vartheta)|^2 \sim \sin^2 2\vartheta \tag{9}$$

has the form of a symmetric dome with a maximum at $\vartheta = 45°$, whereas the dipole component $W_{10}(\vartheta)$ has a maximum at $\vartheta = 90°$. Thus, with allowance for the quadrupole component,

$$W(\vartheta) = a + b\sin^2\vartheta + c\sin^2 2\vartheta. \tag{10}$$

A more complete idea of the physical meaning of the coefficients in (10) and the contribution of the various channels to the angular distribution of the fragments resulting from the photofission of even–even nuclei is given by the relation for the differential cross section

$$2\pi\frac{d\sigma_f(\vartheta)}{d\Omega} \approx \frac{3}{4}\sigma_\gamma^{E1}\left[P_f^{11} + \left(P_f^{10} - \frac{1}{2}P_f^{11}\right)\sin^2\vartheta\right] + \frac{5}{4}\sigma_\gamma^{E2}\left[P_f^{21} + \frac{1}{2}(P_f^{22} - P_f^{21})\sin^2\vartheta + \left(\frac{3}{4}P_f^{20} - \frac{1}{2}P_f^{21} + \frac{1}{8}P_f^{22}\right)\sin^2 2\vartheta\right], \tag{11}$$

in which we use the traditional assumption of predominance of the electric interaction, which is motivated by the circumstance that in the approximation of low multipolarities ($R/\lambda\!\!\!^{-} < 1$)

$$\sigma_\gamma^{M2} \ll \sigma_\gamma^{M1} \approx \sigma_\gamma^{E2} \ll \sigma_\gamma^{E1}, \tag{12}$$

and the contribution of the high-lying states $J^\pi = 1^+$ excited in the case of M1 interaction can be ignored. The fissility P_f^{JK} in the channel with quantum numbers[1] $\lambda = JK$ is defined as

$$P_f^{JK}(E) = \sigma_f^{JK}(E)/\sigma_\gamma^{EJ}(E) \approx T_f(E, E_f^{JK})/T_J(E), \tag{13}$$

where $T_J(E) = \sum_{|K|\leq J} T_f(E, E_f^{JK}) + T_n^J + T_\gamma^J$ is the total penetrability of all decay channels with given spin for both fission [see (8)] and the competing processes, i.e., neutron emission T_n^J and radiative de-excitation T_γ^J.

In studying the influence of the quantum structure of the barrier height E_f^λ on the angular distribution of the fragments (especially in a qualitative analysis of experimental data) it is convenient to consider the ratios of the coefficients (10), which, following the inequalities

$$E_f^{20} < E_f^{10},\ E_f^{J0} < E_f^{JK}, \tag{14}$$

which reflect the content of Bohr's hypothesis, can be represented in accordance with the relation (11) in the form

$$2b/a + 1 \approx T(E, E_f^{10})/T(E, E_f^{11}); \tag{15}$$

$$\frac{c}{b} \approx \frac{5}{4}\frac{\sigma_\gamma^{E2}}{\sigma_\gamma^{E1}}\frac{P_f^{20}}{P_f^{10}} \approx \frac{5}{4}\frac{\sigma_\gamma^{E2}}{\sigma_\gamma^{E1}}\frac{T(E, E_f^{20})}{T(E, E_f^{10})}; \tag{16}$$

$$\frac{T(E, E_f^\lambda)}{T(E, E_f^{\lambda'})} \approx \begin{cases} 1, & E > E_f^{\lambda'}; \\ \exp\left[\frac{2\pi}{\hbar\omega}(E_f^{\lambda'} - E)\right], & E_f^\lambda < E < E_f^{\lambda'}; \\ \exp\left[\frac{2\pi}{\hbar\omega}(E_f^{\lambda'} - E_f^\lambda)\right], & E < E_f^\lambda, \end{cases} \tag{17}$$

where we have assumed that $\hbar\omega < 2\pi(E_f^{\lambda'} - E_f^\lambda)$ and ignored in (16) the difference between the ratios of the fissilities P_f^λ and the penetrabilities $T(E, E_f^\lambda)$ for two channels with different spin and parity combinations. From the relations (15)–(17), we deduce the following properties of the angular distribution of the photofission fragments of even–even nuclei, and they can be regarded as characteristic signs of a "channel" structure of the barrier E_f^{JK} as suggested by Bohr:

1) exponential increase of the ratios (15) and (16) in the region $E_f^\lambda < E < E_f^{\lambda'}$;

2) the existence of an inflection of this dependence in the neighborhood of the energy $E \approx E_f^\lambda$, below which the dependence becomes much weaker or disappears entirely if $\hbar\omega_\lambda = \hbar\omega_{\lambda'}$.

These properties of $W(\vartheta)$ were observed together for the first time in Ref. 16 in a study of ^{238}U photofission induced by a bremsstrahlung beam from the microtron of the Institute of Physics Problems. Figure 3 shows the experimental data and the results of decomposing

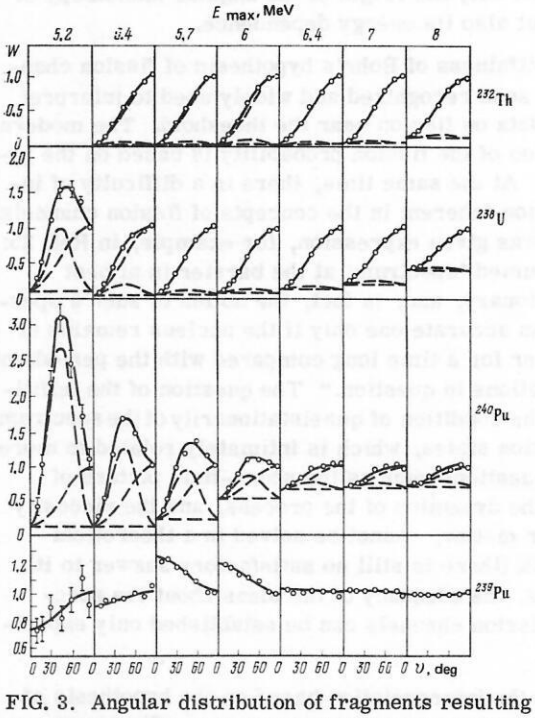

FIG. 3. Angular distribution of fragments resulting from photofission induced by bremsstrahlung γ rays for different electron energies E_{max}.[16–19,31] The broken curves are the components of $W(\vartheta)$.

[1] If channels excited by interactions of the same type, EJ or MJ, are dominant, as in the cases considered here and in what follows, then because of the unique connection between the spin and parity and the set of quantum numbers λ is determined by J and K: $\pi = (-1)^J$ for the EJ interaction and $\pi = (-1)^{J+1}$ for the MJ interaction.

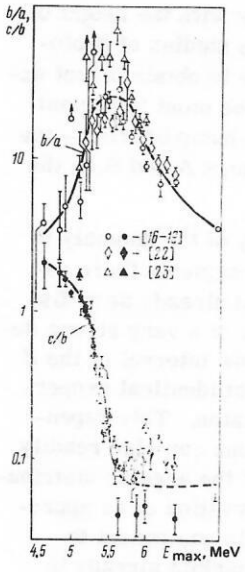

FIG. 4. Experimental dependence of the angular anisotropy (the ratio b/a, open symbols) and the relative contribution of the quadrupole component (c/b, black symbols) for ^{238}U on the limiting energy E_{max} of the bremsstrahlung spectrum. The literature sources are given in square brackets.

$W(\vartheta)$ into components in accordance with (10) obtained in Ref. 16 and from similar measurements for ^{232}Th and ^{240}Pu.[17-19] Despite the difference in the relationships between the components, a common feature for all the nuclei is the qualitative agreement between the energy dependence of their contributions to $W(\vartheta)$ and the prediction expressed by the relations (15)–(17). This is illustrated by means of Fig. 4. A characteristic feature of the dependences in Fig. 4 is the increase in the spread of the data in the region where one of the coefficients becomes too small, namely, a in the upper part and c in the lower part (broken curve). Despite this, it can be clearly seen that the growth in the ratio b/a with decreasing energy stops approximately where the increase in the ratio c/b begins, namely, on the transition through the barrier E_f^{10}, as is required by Bohr's hypothesis and the relations (15)–(17). The decrease in the angular anisotropy of the photofission for $E_{max} \lesssim 5.2$ MeV can be explained by factors which are not associated with the discrete structure of the fission-channel spectrum (see Sec. 3).

For establishing the adequacy of Bohr's model, the information obtained in Ref. 16 on quadrupole photofission has decisive importance. Indeed, before this investigation the very observation of a component proportional to $\sin^2 2\vartheta$ was in dispute,[27] to say nothing of the properties of the ratio c/b from which one could establish the conjectured structure of the spectrum of states of the fissioning nucleus and their connection with the saddle point.

In the sub-barrier region of energies, the exponential decrease of $T(E, E_f^{10})$ compensates the smallness of the ratio $\sigma_f^{E2}/\sigma_f^{E1}$ to such an extent that the quadrupole component c, which can be distinguished with difficulty in $W(\vartheta)$ in the above-barrier region, becomes predominant in the deep sub-barrier region. This mechanism of sub-barrier "enhancement" of the relative contribution of the quadrupole component $W(\vartheta)$, which was first discussed by Griffin,[25] "works" in accordance with (17) only when there is a sufficient distance $E_f^{10} - E_f^{20} > \hbar\omega/2\pi$ between the channels. The distance $E_f^{10} - E_f^{20} \approx 0.6$–$0.7$ MeV (Ref. 17) estimated from the experimental data in Fig. 4 is comparable with the distance between the corresponding levels of heavy nuclei in the ordinary state (of equilibrium deformation). From this, Bohr[28] concluded that there is mirror symmetry of the fissioning nucleus at the saddle point and that the asymmetry of the fission is formed at later stages, i.e., he made more precise the comments quoted above from the pioneering paper.[24] It will be shown below that in the fission process both cases are in fact realized because of the two-hump shape of the barrier, namely, there is symmetry of the saddle point associated with the inner hump and asymmetry of the saddle point associated with the outer hump.

Returning to the experimental verification of Bohr's hypothesis, we can say in summary that the observed energy dependence of the anisotropic components of the angular distribution $W(\vartheta)$ in the region of the threshold not only confirms the expected structure of the photofission-channel spectrum of even–even nuclei, $(J^\pi, K) = (2^+, 0), (1^-, 0), (1^-, 1)$, but also indicates that K is conserved during the fission process, i.e., it is a fairly "good" quantum number, and almost "pure" $D^J_{M,K}$ are observed, namely, the functions $|D^2_{\pm 1,0}(\vartheta)|^2$ and $|D^1_{\pm 1,0}(\vartheta)|^2$. If K mixing were appreciable during the descent from the top of the barrier, it would lead to an appreciable contribution of the isotropic component (for a uniform K distribution, the fission is isotropic).

An angular distribution of the photofission fragments in agreement with the above ideas was studied for eight even–even nuclei from ^{226}Ra to ^{242}Pu.[15-23] The photofission of nuclei with an odd number of nucleons is effectively isotropic.[15,29] This result was also predicted by Bohr,[24] who attributed it to the large number of accessible J states, the lower degree of alignment of the angular momenta due to the presence of the randomly distributed spin of the target nucleus, and the higher density, $E_f^{\lambda'} - E_f^{\lambda} \lesssim \hbar\omega/2\pi$, of the fission channels. An exception is the nucleus ^{239}Pu, which has the minimal spin $\frac{1}{2}$; the angular distribution for it is shown in the lower part of Fig. 3.[30,31]

"Anomalies" in the Z dependence of the ratios b/a and c/b and the two-hump shape of the fission barrier. To illustrate the consequences of Bohr's hypothesis and discuss the experimental data, we used in the previous section a single-hump barrier, as deduced from the liquid-drop model. The dependences of the fissility $P_{10} = \sigma_f^{10}/\sigma_\gamma^{E1} \approx T_{10}/(T_{10} + 2T_{11} + T_\gamma^1)$ and the ratio $b/a = (T_{10} - T_{11})/2T_{11}$ on the excitation energy calculated for such a barrier are shown in the insert to Fig. 5a. One of the properties of these characteristics can be conveniently used in qualitative analysis of experimental data as a characteristic sign of a classical channel structure, namely, in the case of a single-hump barrier the channel effects in the angular anisotropy (the rise and inflection of b/a) must occur in the above-threshold en-

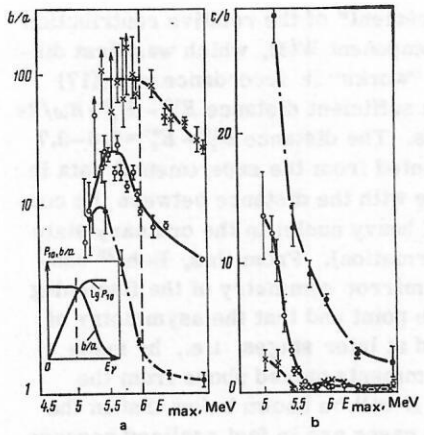

FIG. 5. Dependences of the ratios b/a (a) and c/b (b) on the limiting energy E_{max} of the bremsstrahlung spectrum for the nuclei ^{232}Th (crosses), ^{238}U (open circles), and ^{240}Pu (black circles).[16-19] The broken line shows the position of the observed threshold.

ergy region for the fission cross section.

Data on the angular anisotropy b/a of the fission for three nuclei are given in Fig. 5a. The broken curve shows the position of the observed threshold, which to accuracy 0.2 MeV is the same for these nuclei. It can be clearly seen that the "classical picture" is realized for ^{232}Th but that for the heavier nuclei the position of the inflection in the b/a curve contradicts that picture, being situated not to the right of the observed threshold but to the left, the discrepancy being greater at larger Z of the nucleus. The interpretation of this unexpected property in the framework of the then existing ideas presented serious difficulties,[17,32] and they were overcome only on the basis of the theoretical prediction of the existence of the two-hump shape of the fission barrier of heavy nuclei.[32]

The anomaly in the angular anisotropy of the photofission of even–even nuclei is explained in the framework of the two-hump model as follows.[18,32] For the formation of the angular distribution of the fragments, a new feature of the two-hump model is, as we have already noted, the existence of not one, as before, but two systems of fission channels E^{λ}_{fA} and E^{λ}_{fB}, corresponding to the humps A and B, between which the nucleus can remain, in the well, quite a long time. If this is sufficiently large compared with the K migration period, the nucleus effectively "forgets" through which of the dipole channels, $(1^-, 0)$ or $(1^-, 1)$, it passed in penetrating the inner barrier A, and the anisotropy of the angular distribution of the fragments depends on the channel spectrum at the outer barrier B. Since the threshold observed in the cross section is determined by the height of the largest of the barriers, the expected picture will depend on the ratio of their heights. If the threshold is determined by hump B ($E_{fB} > E_{fA}$), the situation will be close to the one expected in the single-hump model, and it is realized for ^{232}Th(γ, f). In the plutonium isotopes, in particular ^{240}Pu, hump A is higher, so that the channel effects in the angular anisotropy are shifted by the mechanism of "forgetting" (mixing) of K to the sub-barrier energy region of the fission cross section (in accordance with the height of hump B). It was at this stage in the studies of photofission that it first became possible to obtain direct experimental confirmation of one of the most important predictions of the model of the two-hump barrier— the dependence of the heights of the humps A and B on the Z of the fissioning nucleus.[2-4]

With the resolution of the mystery of the anomaly in the angular anisotropy b/a of the fragments there remained another anomaly, which had already been discovered[17] in 1965 and took the form of a very strong dependence of the ratio c/b in a narrow interval of the Z of the nuclei (Th–Pu) despite almost identical properties of the low-lying equilibrium states. This dependence is shown in Fig. 5b, though one can also readily deduce it directly from the form of the angular distributions in Fig. 3. Why does the observation of an appreciable contribution of the quadrupole component to $W(\vartheta)$ in the case of ^{240}Pu become possible already in the region of the threshold, whereas for ^{238}U it is necessary for this to sink in energy into the sub-barrier region and for ^{232}Th it still remains at the $\sigma_\gamma^{E2}/\sigma_\gamma^{E1}$ level deep below the threshold and is barely discernible in Fig. 3? Why is it that for ^{232}Th the mechanism of sub-barrier enhancement of the quadrupole component does not operate but never fails in any of the other investigated cases for six even—even isotopes of uranium and plutonium from ^{234}U to ^{242}Pu (see Refs. 17, 18, 22, 23, and 33), and what is the reason for this anomaly? These questions could only be answered after a further development of the ideas about the fission barrier of heavy nuclei, in particular, the study of the influence on the fission barrier of asymmetric deformations of the type $\alpha_3, \alpha_5, \ldots$.

The calculations of the deformation potential energy by Pashkevich, Möller, Nilsson, and others[9,10] showed that a pear-shaped configuration of the fissioning nucleus with no mirror symmetry corresponds to the energetically most advantageous saddle point of the outer hump B, whereas in passing through the inner hump A and in the second well the configuration of the nucleus preserves mirror symmetry. Depending on the symmetry of the saddle-point configuration, this theoretical prediction implies a change in precisely the part of the spectrum of the low-lying fission channels of even–even nuclei that influences the ratio c/b. As was already noted by Bohr,[24] the loss of reflection symmetry by the nucleus must be accompanied by a significant decrease in the splitting of the $K = 0$ state bands of positive ($K^\pi = 0^+$) and negative ($K^\pi = 0^-$) parity due to the strong dependence of $\hbar\omega_{1\pi v}$ on the barrier height for the tunneling transition between the mirror-reflected configurations. The potential-energy curves are shown schematically as functions of the octupole deformation α_3 for the saddle points A and B in Fig. 6 together with the corresponding fission channels.

It follows from what we have said that the observed picture of the channel effects has a strong dependence on which of the humps of the barrier is higher (Fig. 7); in particular:

a) for the plutonium isotopes, hump A is higher, and

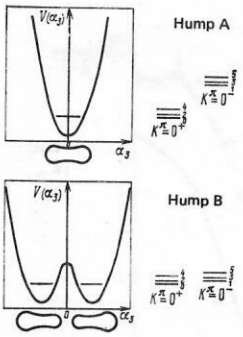

FIG. 6. Positions of the bands of the states of positive and negative parity for a reflection-symmetric nucleus (at hump A) and in the presence of an equilibrium octupole deformation (hump B). The numbers to the right of the lines of the bands indicate the value of J.

it determines the threshold observed in the cross section and, by virtue of the appreciable difference $E_{fA}^{10} - E_{fA}^{20} > \hbar\omega/2\pi$, the "normal" energy dependence of the ratio c/b;

b) for ^{232}Th, hump B is responsible for the threshold observed in the fission cross section and when the nucleus passes through it, it loses its mirror symmetry and with it the $E_{fB}^{10} - E_{fB}^{20}$ splitting and the associated mechanism of sub-barrier "enhancement" of the quadrupole component.

This interpretation, the main ideas of which are due to Vandenbosch,[34] readily explains the dependence of the contribution of the quadrupole component on the Z of the fissioning nucleus, which had long baffled investigators. However, in the framework of this interpretation it was still unclear why in the case of ^{232}Th one does not observe an effect due to the "entrance" of the discrete channels $K^\pi = 0^-$ and then $K^\pi = 0^+$ of the

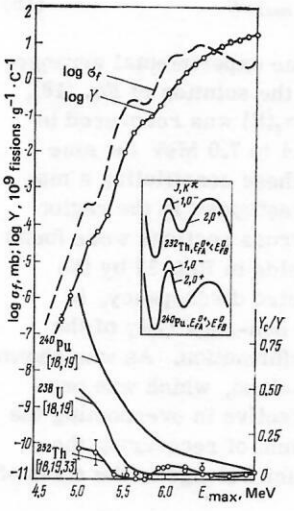

FIG. 7. Energy dependence of the relative contribution of the quadrupole component to the total yield Y_c/Y (at the bottom) and dependence of the yield of the ^{232}Th(γ, f) reaction on the limiting energy of the bremsstrahlung spectrum[37] (at the top). The broken curve is the dependence of the ^{232}Th photofission cross section.[37] The insert shows schematically the structure of the fission barriers of ^{232}Th and ^{240}Pu. The literature sources are given in square brackets.

barrier A when the energy of the γ rays is decreased. The trivial explanation— that the barrier height E_{fA} was not achieved in the measurements— was contradicted by the analysis of other reactions for ^{232}Th and its neighboring isotopes, which led the values $E_{fA} \sim E_{fB} = 6$–6.5 MeV.[8] But apparently this explanation is correct.

It is harder to determine the height of the lower hump for the light actinides ($E_{fA} < E_{fB}$) than it is for the heavy ones ($E_{fA} > E_{fB}$). First, hump A is much narrower (about two times). This effectively rules out the possibility of observing the effect of the "entrance" of the barrier A from a change in the slope of the penetrability curve. Second, there are no such readily identifiable means of decay into the first well as the spontaneous fission of isomers provides for the determination of E_{fB}. Third, and finally, in connection with the prediction of an additional structure of the barrier B, leading to a three-hump potential curve, analysis of resonances of the cross section becomes ambiguous, since in the presence of a third minimum it is not easy to decide the minimum to which the resonances belong. Nevertheless, it was this circumstance that was one of the arguments which made it possible to understand why the previous analysis of sub-barrier resonances and the associated E_{fA} values are unreliable.[8,35]

Thus, there is effectively no experimental information about the A barrier of the thorium nuclei but only the results of theoretical calculations, which systematically show that E_{fA} is less than E_{fB} and less than 5 MeV.[8] The appreciable difference between the spectra of the lowest $K = 0$ channels for the barriers A and B can serve as the property which can, finally, be used to determine the height of barrier A by means of the (γ, f) reaction in this case too. Recently,[36] observation of ^{232}Th has revealed, albeit less clearly than in heavier even–even nuclei but nevertheless quite definite, an increase in the quadrupole component (see Fig. 7), which can be interpreted as the barrier A coming into play. However, estimates of E_{fA}^{10} and E_{fB}^{20} from the behavior of the c/b curve are prevented by the strong resonance structure of the penetrability of both channels. For this purpose, we require experimental data on the angular distribution of the fragments at even lower eneriges $E_{max} < 5$ MeV of the γ rays.

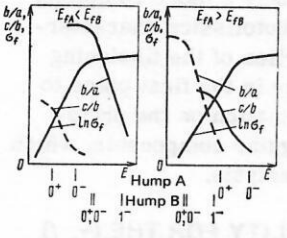

FIG. 8. Structure of the lowest K^π channels at the humps A and B (lower part of the figure) for $E_{fA} < E_{fB}$ and $E_{fA} > E_{fB}$; the behavior of the photofission cross section and of the main characteristics b/a and c/b of the fragment angular distribution due to this structure. The continuous curves in the main part of the figure show the characteristics determined by the higher of the humps.

Figure 8 shows schematically (without allowance for resonance effects under the assumption that K is "forgotten" in the second well) the properties of the most important characteristics of the photofission probability of even–even heavy nuclei. The left-hand figure illustrates the extreme situation characteristic for ^{232}Th and lighter nuclei that is realized in the case of a sufficient difference $E_{fA} - E_{fB} < 0$ between the heights of the barriers. It corresponds basically to the picture discussed by Bohr for a reflection-symmetric nucleus when the dipole photofission channels are predominant in the region of the threshold. As the difference $E_{fA} - E_{fB}$ increases, the growth of the ratio c/b associated with the channels of barrier A is shifted to the threshold observed in the cross section and the increase in the ratio b/a associated with the channels of barrier B is, conversely, shifted to the sub-barrier energy region. With increasing Z (i.e., as we pass from thorium to plutonium), the energies at which the increase in the two ratios is observed not only approach each other [this tendency is confirmed by the experiment in the Th–Pu region (see Figs. 5a and 5b)] but actually change places. This corresponds to the picture of the channel effects shown in the right-hand part of Fig. 8, which arises when the difference between the heights of the humps A and B is so great that $E_{fA}^{20} > E_{fB}^{11}$. It may be encountered in the as yet unstudied Cm or Cf nuclei with $E_{fA} - E_{fB} > 1$ MeV.

It can be concluded that the experimental data on the angular distribution of the fragments from photofission are, by virtue of the simplicity of the spectrum of the accessible channels, extremely informative about the spectrum of the transition states, the shape of the barrier, and the symmetry of the nuclear configuration at different stages of the process. To demonstrate this advantage of the (γ, f) reaction most clearly, we have deliberately made only a qualitative analysis, restricting the discussion to the characteristic features of the experimentally investigated quantities. Note that these are integral quantities, being averaged over the bremsstrahlung continuum, which washes out the resonance structure of the cross sections that is also associated with the quantum states of the fissioning nucleus but in the wells rather than at the tops of the barriers. The analysis of the averaged structure made it possible to simplify the picture and identify in it the effects due to the discrete nature of the fission-channel spectrum. It is interesting to make a more complete, quantitative description of the photofission characteristics, combining all the properties of the fissioning system. For this it is necessary in the first place to consider the experimental information on the photofission cross section and its angular components, which are the direct subject of such analysis.

2. CROSS SECTION AND FISSILITY FOR THE (γ, f) REACTION IN THE REGION OF THE THRESHOLD

Photofission cross section of the actinides. There have been only a few[15,18,37] systematic and detailed investigations of sub-barrier and near-threshold photofission of heavy nuclei. Figures 9 and 10 show the results of Ref. 37, in which the yield

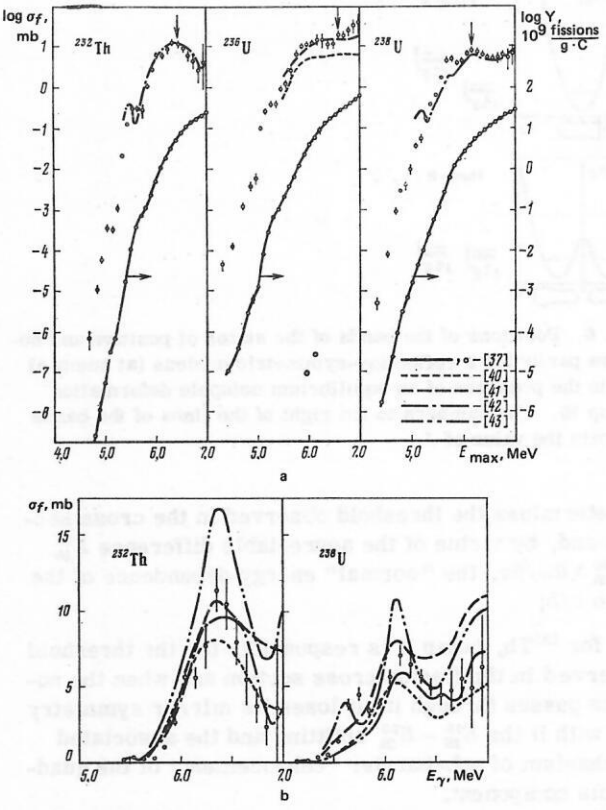

FIG. 9. Yield $Y(E_{max})$ and cross section of the photofission reaction of the nuclei ^{232}Th, ^{236}U, and ^{238}U (a), and a comparison of the dependences $\sigma_f(E_\gamma)$ for ^{232}Th and ^{238}U as obtained in experiments with a bremsstrahlung beam (the points) and using quasimonochromatic γ rays (b). In Figs. a and b the designation of the curves is the same. The arrows at the top indicate the position of the threshold of the (γ, n) reaction. The literature sources are given in square brackets.

$$Y(E_{max}) = c \int_0^{E_{max}} \sigma_f(E)\, N(E, E_{max})\, dE \qquad (18)$$

was measured and, for the same experimental arrangement, in a unified approach to the solution of Eq. (18), the photofission cross section $\sigma_f(E)$ was recovered in the range of energies[2)] from 4.4 to 7.0 MeV for nine nuclides from ^{232}Th to ^{241}Am, these constituting a majority (2/3) of the actinides investigated in the region of the fission threshold. The cross sections were found from the measured integral yields in Ref. 37 by the method of minimizing the directed discrepancy, in which the physical condition of non-negativity of the solutions is used as *a priori* information. As was shown by test calculations,[37,38] this method, which was proposed by Tarasko,[39] is very effective in overcoming the difficulties in solving the problem of recovering the photofission cross section, which belongs to the class of improperly posed problems.

The curves in Figs. 9 and 10 show the results of other studies, in which various methods were used to mono-

[2)] The energy of the γ rays, like the excitation energy, equal to it, of the compound nucleus, is denoted by E, and in some figures by E_γ. In Figs. 9a, 10, and 21 a common scale of the energies E_{max} and E is given.

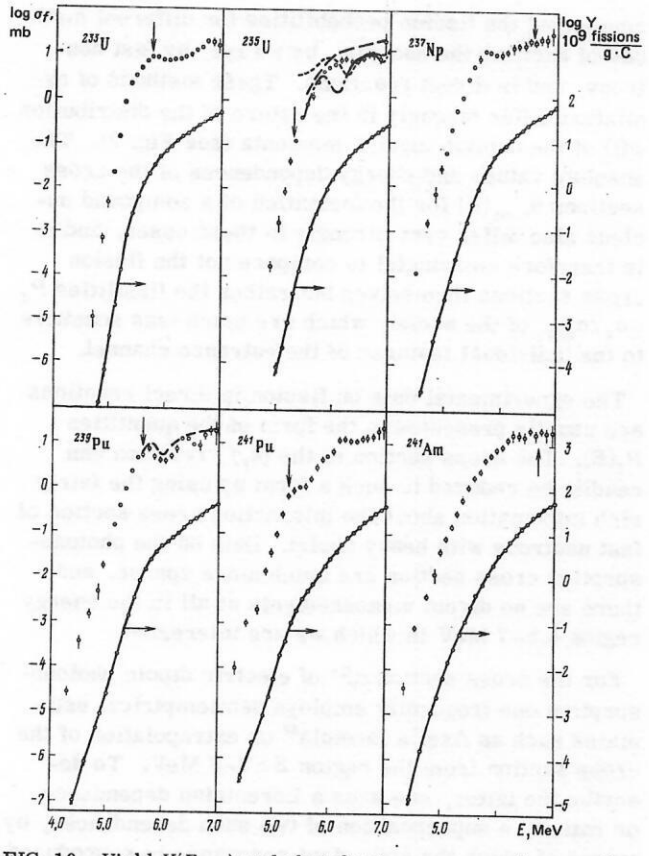

FIG. 10. Yield $Y(E_{max})$ and photofission cross section σ_f of odd nuclei investigated in Ref. 37. The notation is as in Fig. 9.

chromatize the γ rays.[40-43] The best studied cases (^{232}Th, ^{238}U) are shown in Fig. 9b. The experimental data reveal a resonance structure, despite the discrepancy (by about a factor 2) in the results of the measurement of $\sigma_f(E)$ by the individual groups. It can also be seen that the weak intensity of the quasimonochromatic γ rays significantly restricts the applicability of the corresponding methods at low energies. In addition, the very concept of monochromatization is rather formal; in Refs. 40–43, the energy resolution of the γ rays was 200–300 keV.

The data obtained on the fission cross section indicate that the nucleon composition of the fissioning nucleus has a strong influence on the properties of the fission barrier.

1. Compared with the photofission cross section of even–even nuclei (see Fig. 9), the cross sections for odd nuclei (see Fig. 10) are much steeper in the sub-barrier region of energies. This property is usually attributed to the influence of the parity of the number of nucleons on the mass parameter which determines the curvature parameter in Eq. (8).

2. The steepness of the log σ_f curves in the sub-barrier region decreases appreciably with increasing Z of the fissioning nucleus. As is shown in Fig. 11, this behavior, which is in sharp contradiction to the results of calculations in the framework of the liquid-drop model, can be explained by a two-hump shape of the fission barrier of heavy nuclei and different curvatures

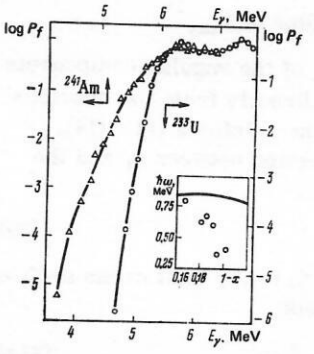

FIG. 11. Comparison of the energy dependences of the fissilities of ^{233}U and ^{241}Am (Ref. 37) and comparison of the effective curvature parameter $\hbar\omega \approx 2\pi(d \ln P_f/dE)^{-1}$ (the points) with calculations in accordance with the liquid-drop model[86] (continuous curve). Here, $x = (Z^2/A)/(Z^2/A)_{crit}$ is the fissility parameter, where $(Z^2/A)_{crit}$ is taken equal to 45.

of its humps. Thus, the rapid decrease of $\sigma_f(E)$ in the case of the lightest nuclei (the smallest values of $\hbar\omega$ in Fig. 11) is associated with tunneling through both humps, whereas for the heavier nuclei, for example, ^{241}Am, it is due solely to the penetrability of the higher and narrower inner hump.[44,45]

3. The photofission cross section of even–even nuclei has a much more pronounced resonance structure, which is explained by the lower density of the internal excitation states, to which the vibrational motion in the second well is coupled, and the smaller number of fission channels compared with odd nuclei.

Despite these differences between the fission barriers and the resulting properties of the cross sections, the threshold observed in them (the height E_f^{max} of the higher hump) differs little from nucleus to nucleus, as was already mentioned in the previous section. This is explained by the influence of the nucleon shells on the deformation potential energy of the nucleus during the fission process.[5] The properties of the photofission probability noted above and their consequences for the fission barrier agree with the results of investigation of an even larger number of nuclei in direct reactions.[44-46]

The position of the threshold of the (γ, n) reaction was calculated from the binding energy B_n from Ref. 47. As a rule, the values of B_n are correlated with the irregularities of the fission cross section, namely, the dips in the region of the plateau for N-even nuclei ($B_n > E_f^{max}$) and the decrease in the steepness in the sub-barrier region for N-odd nuclei ($B_n < E_f^{max}$), a phenomenon which is due to the competition between fission and neutron emission.

Angular components of the photofission cross section. Besides the photofission cross section $\sigma_f(E)$, its angular components $\sigma_a(E)$, $\sigma_b(E)$, and $\sigma_c(E)$ are also of considerable interest. Like the total cross section

$$\sigma_f = \sigma_a + \sigma_b + \sigma_c,$$

they can be recovered using the integral equation (18) from the corresponding components of the total yield:

$$Y_a = \frac{a}{\nu} Y;\ Y_b = \frac{2}{3}\frac{b}{\nu} Y;\ Y_c = \frac{8}{15}\frac{c}{\nu} Y;\ \nu = a + \frac{2}{3} b + \frac{8}{15} c, \quad (19)$$

where Y_i, Y, a, b, c are functions of E_{max}.

The physical interpretation of the angular components of the cross section follows directly from the previous section, specifically, from the relations (11)–(14), which readily yield the connection between σ_i and the partial cross sections

$$\sigma_f^{JK} = \sigma_\gamma^{EJ} P_f^{JK}, \tag{20}$$

which express the contribution to the total cross section of the specific fission channels:

$$\sigma_a = \tfrac{3}{2}\sigma_f^{11} + \tfrac{5}{2}\sigma_f^{21} \approx \tfrac{3}{2}\sigma_f^{11}; \tag{21a}$$

$$\sigma_b = \sigma_f^{10} - \tfrac{1}{2}\sigma_f^{11} + \tfrac{5}{6}(\sigma_f^{22} - \sigma_f^{21}) \approx \sigma_f^{10} - \tfrac{1}{2}\sigma_f^{11}; \tag{21b}$$

$$\sigma_c = \sigma_f^{20} - \tfrac{2}{3}\sigma_f^{21} + \tfrac{1}{6}\sigma_f^{22} \approx \sigma_f^{20}. \tag{21c}$$

The approximate equalities in the last relations are obtained when the small quadrupole terms are ignored compared with the dipole terms in σ_a and σ_b and when allowance is made for the predominance of the $K = 0$ channel in σ_c near the threshold. In this approximation, the components of the cross section can be determined for all the most important photofission channels of even–even nuclei. In the channel analysis of the fission probability, this possibility is an exceptionally important factor, and its significance will be demonstrated in what follows.

Figure 12 shows the energy dependences of the quadrupole component of the cross section and the angular anisotropy of photofission

$$b/a = W(90°)/W(0°) - 1 = (3/2)\,\sigma_b(E)/\sigma_a(E)$$

as recovered from the results of measurements of $Y(E_{max})$, $a(E_{max})$, $b(E_{max})$, and $c(E_{max})$ for ^{238}U. They are compared with the analogous quantities measured directly in experiments with monoenergetic γ rays.[17,48-51] It follows from the information contained in Figs. 9 and 12 that the possibilities of modern methods of obtaining monochromatic γ rays are very restricted as regards the intensity, and that as yet there is no alternative to bremsstrahlung beams for study of sub-barrier excitation energies.

Cross sections of electric dipole and quadrupole photoabsorption. There is considerable interest in comparing the fission probabilities for different methods of exciting the nucleus: by γ rays, by fast neutrons, and in direct reactions. These methods of excitation differ strongly in the nature of the distribution $\varphi(l)$ of the orbital angular momenta (see Fig. 2). The absolute values and energy dependences of the cross sections $\sigma_{comp}(E)$ for the formation of a compound nucleus also differ very strongly in these cases, and it is therefore meaningful to compare not the fission cross sections themselves but rather the fissilities $P_f = \sigma_f/\sigma_{comp}$ of the nuclei, which are much less sensitive to the individual features of the entrance channel.

The experimental data on fission in direct reactions are usually presented in the form of the quantities $P_f(E)$. The cross section of the (n,f) reaction can readily be reduced to such a form by using the fairly rich information about the interaction cross section of fast neutrons with heavy nuclei. Data on the photoabsorption cross section are much more sparse, and there are no direct measurements at all in the energy region 4.5–7 MeV in which we are interested.

For the cross section σ_γ^{E1} of electric dipole photoabsorption one frequently employs semiempirical estimates such as Axel's formula[52] or extrapolation of the cross section from the region $E > 7$–8 MeV. To describe the latter, one uses a Lorentzian dependence, or rather, a superposition of two such dependences, by means of which the split giant resonance is reproduced.

Figure 13 shows the most detailed data on the photoabsorption cross section for heavy nuclei at $E \leq 10$ MeV. In Ref. 53, they were obtained by the transmission method, and in Refs. 41 and 54 by adding the partial cross sections for the main competing processes (fission and neutron emission), i.e., under the assumption that $\sigma_\gamma \approx \sigma_f + \sigma_{\gamma n}$. In this case, no allowance is made for the contribution of radiative de-excitation of the compound nucleus, which, because of the smallness and

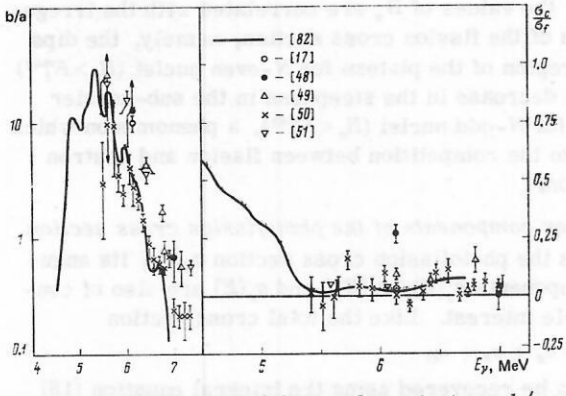

FIG. 12. Dependences of the angular anisotropy b/a and the quadrupole component σ_c/σ_f of the total cross section of ^{238}U photofission on the energy of the γ rays. The literature sources are given in square brackets.

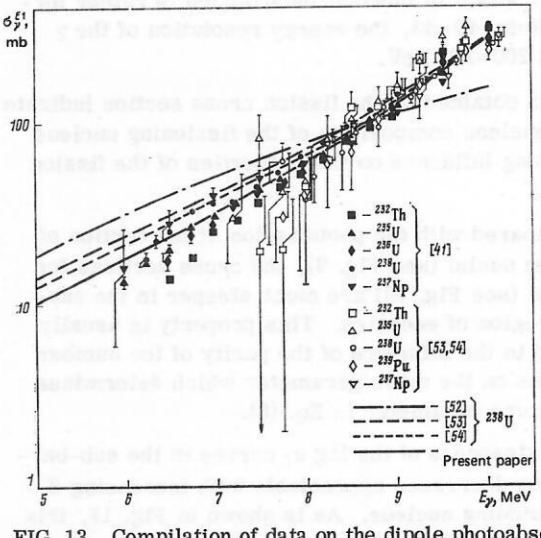

FIG. 13. Compilation of data on the dipole photoabsorption cross section σ_γ^{E1}. The continuous curve is the result of fitting the data of Ref. 41 in accordance with Eq. (22) in the region $E_\gamma = 6$–10 MeV. The literature sources are given in square brackets.

weak energy dependence of the radiative widths, can be ignored at sufficiently high excitation energies above the thresholds of fission, E_f, or neutron emission, B_n. Through the data, we have drawn a smooth curve (the continuous curve in Fig. 13) and used it to calculate the fissilities plotted in Fig. 15. The curve was obtained by fitting the data in the region $E = 6$–10 MeV by a superposition of the two Lorentzian curves

$$\sigma_\gamma^{E1}(E) = \sum_{i=1,2} \sigma_i \frac{(\Gamma_i E)^2}{(E^2 - E_i^2)^2 + (\Gamma_i E)^2} \qquad (22)$$

with the parameters $\sigma_1 = 250$ mb, $E_1 = 10.5$ MeV, $\Gamma_1 = 2.5$ MeV, $\sigma_2 = 300$ mb, $E_2 = 14$ MeV, $\Gamma_2 = 4.5$ MeV.

These parameters differ appreciably from those that ensure a description of the giant resonance. Conversely, the parameters which give the best description of the giant resonance lead to a significant overestimation of σ_γ^{E1} in the rather long extrapolation of (22) in which we are interested.

Until recently, the only source of information about the electric quadrupole absorption of γ rays by heavy nuclei was provided by data on quadrupole photoabsorption,[18,19] from which an estimate was obtained for the ratio of the cross section of electric dipole photoabsorption to that for electric quadrupole absorption, $\sigma_\gamma^{E1}/\sigma_\gamma^{E2} \approx 25$–$30$, this being in satisfactory agreement with electrodynamic calculations. The shape of the energy dependence of the cross section of quadrupole photoabsorption was usually taken to be the same as for dipole absorption.

In recent years, new experimental data (see, for example, the reviews of Refs. 55 and 56) have indicated the existence of "new giant resonances," in particular, a resonance at $E = (60$–$65)A^{-1/3}$ MeV (A is the mass number). It is assumed that it can be identified as an isoscalar electric quadrupole resonance. The appearance of this resonance in the cross section of quadrupole photoabsorption by the nucleus ^{238}U is noted in Refs. 57–59.

Figure 14 shows the Lorentzian energy dependences of the quadrupole photoabsorption cross section calculated with the parameters of the Lorentzian curves recommended in Refs. 57–59. In Ref. 58, the resonance was excited in the reaction $^{238}U(e, e'\alpha)$; in Ref. 59, in

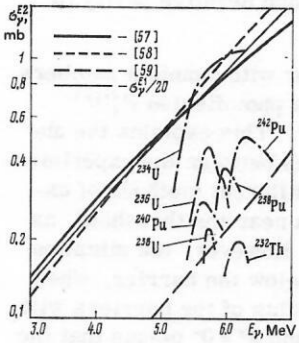

FIG. 14. Compilation of data on the quadrupole photoabsorption cross section σ_γ^{E2}. The continuous (heavy) and broken curves are the results of calculation in accordance with Eq. (23). The literature sources are given in square brackets.

the reaction $^{238}U(e, e')$. For comparison with photofission, particularly interesting data were obtained in Ref. 57, in which $^{238}U(e, e'f)$ electrofission was investigated; the point is that in the spectrum of virtual photons the E2 component is much more intense than the E1 component.[60] In the spectrum of the real photons, the components of all multipolarities are equally represented. The chain curves in Fig. 14 show the quadrupole photofission cross sections obtained in experiments with bremsstrahlung γ rays. For the nuclei ^{232}Th, ^{238,240,242}Pu, the results of Ref. 18 were used; for ^{234}U, the results of Ref. 22; and for ^{236,238}U, the results of Refs. 22 and 33. It can be seen from the figure that the parameters of Ref. 59 give low cross sections in disagreement with the photofission data and Refs. 57 and 58. In the energy region below 7 MeV in which we are interested, the cross sections in Refs. 57 and 58 are approximately the same, do not contradict the photofission data, and correspond to $\sigma_\gamma^{E1}/\sigma_\gamma^{E2} \approx 20$ for our adopted value of σ_γ^{E1} (see Fig. 14). In the present paper, we have used the Lorentzian energy dependence

$$\sigma_\gamma^{E2}(E) = \sigma_m \frac{(\Gamma_m E)^2}{(E^2 - E_m^2)^2 + (\Gamma_m E)^2}$$

for the cross section of electric quadrupole photoabsorption with parameters from Ref. 57: $\sigma_m = 2.8$ mb, $E_m = 9.9$ MeV, $\Gamma_m = 6.8$ MeV.

Influence of the method of excitation on the fissility. The estimates obtained in the previous section for the components of the photoabsorption cross section make it possible to compare the fissilities of heavy nuclei in the region of the threshold for the different methods of excitation used in this energy region— in the reactions (γ, n) and (n, f) and in the direct reactions (t, pf), (d, pf), etc. This question has been discussed in a number of papers, for example, Refs. 61 and 62, and in most detail in Ref. 37. We shall consider only the most interesting examples and the consequences that flow from them.

In Fig. 15, we give the experimental data on the fissilities of the nuclei for which the yield and photofission cross section were studied in Ref. 37. In all the cases above the threshold and for four of the five odd nuclei (the exception is ^{239}Pu) in the sub-barrier energy region, the fissilities are in satisfactory agreement despite the difference in the kinematics of the compared reactions. It can be concluded from this that in the indicated situations the number of accessible channels is sufficiently large for the observed fissility

$$P_f = \left(\sum_{J,\pi} \alpha_{J\pi} P_f^{J\pi}\right) / \sum_{J,\pi} \alpha_{J\pi} \qquad (24)$$

to depend weakly on the differences in the $\varphi(l)$ distributions of the entrance channel (see Fig. 2) which, together with the spin of the target nucleus, determine the excitation spectrum $\alpha_{J\pi}$ of the compound nucleus.

The resonances of the fission penetrability may lead to a clearer manifestation of the states than the discrete structure of the fission-channel spectrum, especially if $\Delta E_f^{\lambda\lambda'} \approx \hbar\omega/2\pi$, as in the considered case of odd nuclei. We evidently encounter such a situation in the $^{239}Pu(\gamma, f)$ reaction. It is unique in the sense that in it,

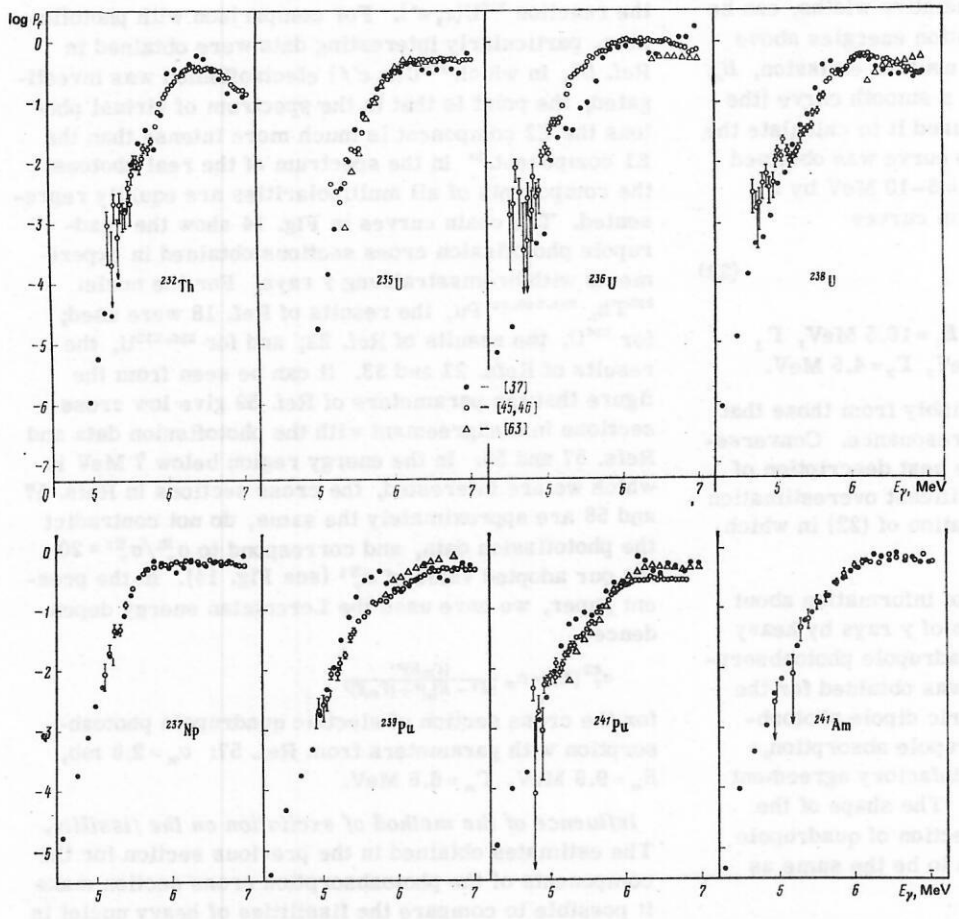

FIG. 15. Fissility P_f in (γ, f) reactions (circles) and in direct reactions (triangles). The literature sources are given in square brackets.

because of the spin $1/2^+$ of the target nucleus, the smallest set of compound states, $J^\pi = 1/2^-$ and $3/2^-$, is realized among all the cases of photofission of odd nuclei, and, as is shown by the analysis in Ref. 31, the penetrability of the channel $K^\pi = 3/2^-$ has a resonance at $E = 5.6$ MeV, which can be clearly seen in Figs. 10 and 15. The participation in the reaction ^{238}U(n, f) in this region of energies of the $J^\pi = K^\pi = 1/2^+$ channels, which are excited by s neutrons, and of other channels in the reaction ^{238}Pu(d, pf), reduces the importance of the $J^\pi = 3/2^-$ states in P_f compared with the (γ, f) reaction.

Of even greater interest in connection with the specific predictions that follow from Bohr's hypothesis about the spectrum of the fission channels is a comparison of data on the fissilities of even–even nuclei, particularly for the (γ, f) and (t, pf) reactions, in which the quantum numbers $\alpha_{J\pi}$ of the populated compound states are determined by the single selection rule $J = l$, $\pi = (-1)^l$. An important difference between the reactions is that whereas bands of channels (for even–even nuclei, the $K^\pi = 0^+$ and 0^- channels) participate in the fission process near the threshold after the direct reaction on account of the wide distribution $\varphi(l)$ of the transferred angular momenta, in the case of photofission only one of them, $J^\pi = 2^+$ and 1^-, participates. Near the threshold, the fissilities in these reactions can be represented as

$$P_f^{(\gamma, f)} = \frac{\sigma_\gamma^{E1} P_f^- + \sigma_\gamma^{E2} P_f^+}{\sigma_\gamma^{E1} + \sigma_\gamma^{E2}} \approx P_f^- + \frac{\sigma_\gamma^{E2}}{\sigma_\gamma^{E1}} P_f^+; \quad (25)$$

$$P_f^{(t, pf)} = (\alpha^+/\alpha)\, P_f^+ + (\alpha^-/\alpha)\, P_f^- \approx (1/2)\,(P_f^+ + P_f^-), \quad (26)$$

where P_f^+ and P_f^- are the fissilities for the individual channels with quantum numbers $K^\pi = 0^+$ and 0^-, which, for simplicity, are taken to be the same within one band; $\alpha^+ = \sum_{J;\pi=+1} \alpha_{J\pi}$; $\alpha^- = \sum_{J;\pi=-1} \alpha_{J\pi}$. The last approximation in (26) corresponds to the assumption of equal probabilities of population of the states of the compound nucleus of positive and negative parity (α^+ and α^-).

At energies above the barrier with quantum numbers $K^\pi = 0^-$, $P_f^+ \approx P_f^- \approx P_f^{(t, pf)}$, and in photofission $P_f^{(\gamma, f)} \approx P_f^- \approx P_f^{(t, pf)}$ because $\sigma_\gamma^{E2} \ll \sigma_\gamma^{E1}$. This explains the absence of significant differences between the experimental data on the fissilities for different methods of excitation of the fission reaction near the threshold, as was already noted in Ref. 61. However, the situation must change sufficiently far below the barrier, when the difference between the heights of the barriers with the quantum numbers $K^\pi = 0^+$ and $K^\pi = 0^-$ means that the ratio P_f^+/P_f^- increases appreciably. This is readily seen by considering the limiting case corresponding to an inequality $P_f^- \ll P_f^+$ so strong that P_f^- can be ignored compared with $P_f^+ \sigma_\gamma^{E2}/\sigma_\gamma^{E1}$. It then follows from

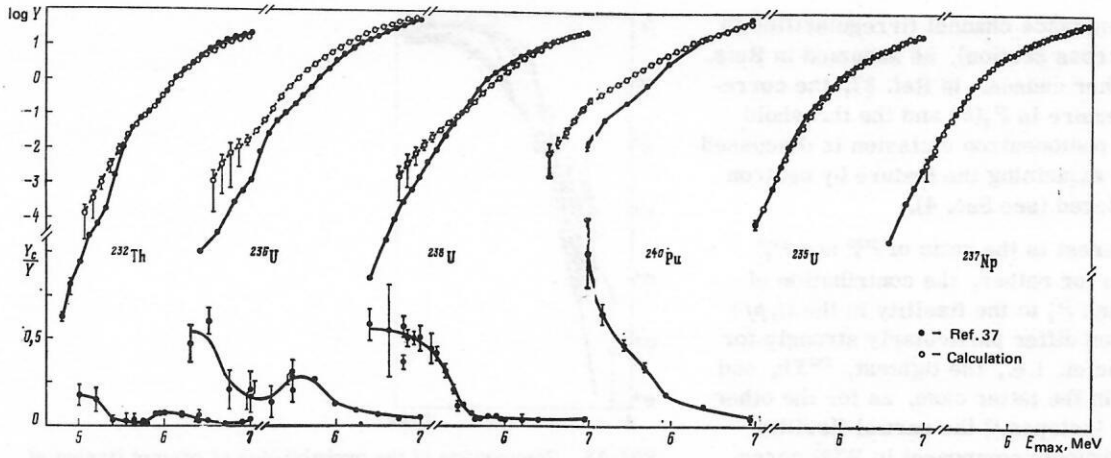

FIG. 16. Comparison of the yields of the (γ, f) reaction with the results of calculations in accordance with Eq. (18) in which $\sigma_f = \sigma_\gamma^{E1} P_f^{t, pf}$. The data on the fissility in the (t, pf) reaction are taken from Refs. 45 and 46 for ^{237}Np, we have used the data of Ref. 45 on the reaction ^{236}U(^{3}He, df)^{237}Np. At the bottom of the figure, we show the experimental data on the relative contribution of the quadrupole component ot the total yield of the photofission reaction.[18,19,33,36]

(25) and (26) that

$$P_f^{(t,\ pf)}/P_f^{(\gamma,\ f)} \approx \sigma_\gamma^{E1}/2\sigma_\gamma^{E2} \gg 1, \qquad (27)$$

i.e., the fissility in the (t, pf) reaction may exceed the photofissility by about an order of magnitude. In the general case, there must be a correlation with the contribution of the quadrupole photofission.

For some nuclei, Fig. 16, which is taken from Ref. 37, gives (in the lower part of the figure) data on the relative contribution of the quadrupole component to the total yield:

$$\frac{Y_c}{Y} = \frac{8}{15}c \Big/ \left(a + \frac{2}{3}b + \frac{8}{15}c\right).$$

The upper part of the figure gives data on the yield itself, which is compared with the analogous quantity obtained from the observed fissility[45,46] by integrating the cross section, equal to $\sigma_\gamma^{E1} P^{(t, pf)}$, over the bremsstrahlung spectrum. The data on the yield for even–even nuclei above the threshold as well as for the odd nuclei in the entire overlapping energy region agree, in connection with which we note that no normalization of the "constructed yield" to the measured yield of the (γ, f) reaction was made. The correlation between the dependences given in Fig. 16 is very clear: Wherever the contribution of Y_c to Y is appreciable in the sub-barrier energy region the "yield" $Y^{(t, pf)}$ deviates from Y, as is required by the relation (27). The comparison is particularly effective in the extreme cases of ^{240}Pu, for which the contribution of Y_c to Y and the deviation of $Y^{(t, pf)}$ from Y are both already appreciable near the threshold (around 6 MeV) and rapidly increase with decreasing energy, and ^{232}Th, where a small effect is noted only far below the threshold and near the sensitivity limits of the methods of measuring $P_f^{(t, pf)}$ and $W(\vartheta)$ in the (γ, f) reaction.

From the experimental data on the angular components of the photofission cross section and the estimates of σ_γ^{E1} and σ_γ^{E2} in accordance with (20) and (21), it is possible to recover the partial fissilities $P_f^{20} \approx P_f^+$ and $P_f^{10} \approx P_f^-$ of even–even nuclei, and these make possible a more detailed comparison of the fission probabilities in the (γ, f) and (t, pf) reactions than from analysis of the integral characteristics. Figure 17 shows the energy dependences of $P_f^{(t, pf)}$ (Ref. 46), P_f^{20}, and P_f^{10} for the four nuclei considered above: ^{232}Th, ^{236}U, ^{238}U, and ^{240}Pu. In discussing them, it must be borne in mind that it is not so much the comparison of the absolute values of the fissilities, which, as we have already mentioned, may have appreciable errors of measurement for the (γ, f) reaction, which is informative, but rather the new data, obtained from photofission, on the distribution of the fissility observed in the direct reaction over the individual bands of the channels. From this point of view, the agreement between the energy dependences in Fig. 17 (overall and in many details) is very heartening. For example, the two groups of data have resonances at coincident energies, and the data of the (γ, f) reaction readily permit identification of the quantum numbers K^π, namely, 0^- for ^{232}Th at 5.5 MeV, 0^+ for ^{236}U at 4.6 MeV, 0^+ for ^{238}U at 5.1 MeV, 0^- at 5.8 MeV, and 0^+ for ^{240}Pu at 5.1 MeV. The presence of the broad maximum in the fissility of ^{238}U at 6.2 MeV (see also Fig. 15) independently of the method of excitation indicates that the effect is not due

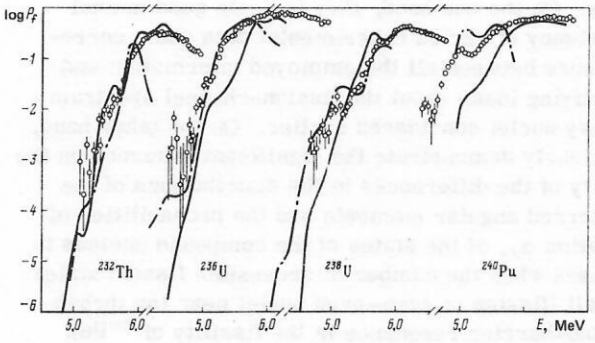

FIG. 17. Comparison of the fissilities of the nuclei ^{232}Th, ^{236}U, ^{238}U, and ^{240}Pu in the reactions (t, pf) (circles[46]) and (γ, f) (continuous curve for dipole photofission, chain curve for quadrupole photofission[18,89]).

to properties of the entrance channel (irregularities in the photoabsorption cross section), as assumed in Refs. 64 and 65, but has other causes. In Ref. 37, the correlation between this feature in $P_f(E)$ and the threshold $E = B_n = 6.14$ MeV for photoneutron emission is discussed and the possibility of explaining the feature by neutron competition is considered (see Sec. 4).

Of considerable interest is the ratio of P_f^{20} and P_f^{10} and their contribution (or rather, the contribution of the nearly equal P_f^+ and P_f^- to the fissility in the (t, pf) reaction. The pictures differ particularly strongly for the two "extreme" nuclei, i.e., the lightest, ^{232}Th, and the heaviest, ^{240}Pu. In the latter case, as for the other even–even plutonium isotopes,[18] the partial fissility P_f^{20} [to which the quadrupole component in $W(\vartheta)$ corresponds] predominates right from the threshold observed in the dipole cross section at $E \approx 6$ MeV, whereas for ^{232}Th the cross section decreases by five orders of magnitude as E varies from 6 to 5 MeV, and $P_f^{20} \approx P_f^{10}$ apart from resonance effects. As was shown above in connection with the discussion of the Z dependence of the quadrupole component in the angular distribution of the fragments, this effect can be explained by the change in the symmetry of the fissioning nucleus on the transition from the inner to the outer hump and the difference between their heights E_{fA} and E_{fB}.

We recall that in the first transition state (at hump A) the nucleus is reflection-symmetric, and, like an ordinary nucleus with equilibrium deformation, has a barrier-height difference $E_{fA}^{0^-} - E_{fA}^{0^+} = \hbar\omega_0$, where $\hbar\omega_0$ is the energy of the octupole vibrations. At the larger deformation in the second transition state, the nucleus loses its reflection symmetry, and with it the energy splitting between the $K^\pi = 0^+$ and 0^- bands that ensures the difference between P_f^{20} and P_f^{10}. In the ^{240}Pu nucleus, hump A is approximately 1 MeV higher than hump B, but in ^{232}Th the situation is reversed, which explains the observed dependence of $P_f^{20}/P_f^{10} \sim c/b$ on the Z of the fissioning nucleus. The characteristic features of the fission barriers and the spectra of the transition states of these nuclei are shown schematically in Fig. 7. In particular, the figure idealizes the effect of the static reflection-asymmetric deformation—it is assumed that $E_{fB}^{0^-} - E_{fB}^{0^+} = \hbar\omega_{inv} - 0$.

The results of this analysis are important in two respects. On the one hand, they indicate good mutual consistency of varied experimental data and a correspondence between all the employed information and the unifying ideas about the fission-channel spectrum of heavy nuclei considered earlier. On the other hand, they clearly demonstrate the significant influence on the fissility of the differences in the distributions of the transferred angular momenta and the probabilities of population $\alpha_{J\pi}$ of the states of the compound nucleus in the cases when the number of accessible fission states is small (fission of even–even nuclei near the threshold, sub-barrier resonance in the fissility of ^{239}Pu). We shall give one further example of unexpected influence of the entrance channel of the reactions on the fissility of nuclei; it is evidently due to the fact that the target nucleus has spin.

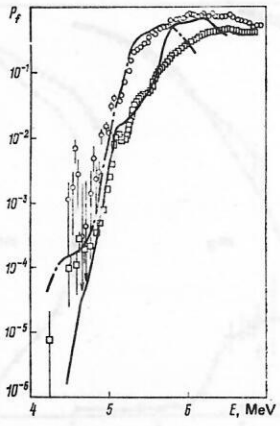

FIG. 18. Comparison of the probabilities of prompt fission of the nucleus ^{236}U in the reactions (t, pf) (circles[46]), (d, pf) (rectangles[66]), and (γ, f) (the continuous and the chain curves are for dipole and quadrupole photofission[89]).

Figure 18 shows the fissility in the ^{235}U(d,pf) reaction[66]; its values in the threshold region of energies are several times smaller than the fissility of the same compound nucleus ^{236}U in the ^{234}U(t, pf) and ^{236}U(γ, f) reactions. The same difference in $P_f(E)$ for the (d,pf) and (t, pf) reactions is revealed by a comparison of the experimental data[44,46] for other even–even nuclei, namely, ^{240}Pu, ^{242}Pu, and ^{248}Cm, and the scale of the effect is correlated with the spin of the target nucleus in the (d, pf) reaction. At the same time, the fissilities of the odd nucleus ^{241}Pu in the ^{240}Pu(d, pf) and ^{239}Pu(t, pf) reactions are nearly equal,[44,46] which, as we have already noted in connection with the discussion of Fig. 15, is characteristic of the nuclei of this type. This suggests that the effect occurs only for even–even nuclei, and, since it is maximal in the region of the threshold, where the $K = 0$ channels play the predominant part in the (γ, f) and (t, pf) reactions, the decrease in the fissility in the (d, pf) reaction must be attributed to the suppression of the contribution of precisely these channels.

There is direct experimental evidence which shows that the $K = 0$ channels are suppressed when even–even nuclei produced from odd target nuclei with high spin undergo fission and that the effect is not restricted to the (d, pf) process. We are referring to the angular distribution of the fragments from the fission of oriented ^{235}U$(7/2^-)$ and ^{233}U $(5/2^+)$ nuclei by slow neutrons,[67,68] which makes it possible to determine the contribution of the channels with different K for many states of the compound nucleus (neutron resonances) with known spins J. At all J, the K distributions recovered from these data reveal a predominance of $K \neq 0$, apparently contradicting the existing ideas about the fission-channel spectrum of even–even nuclei. Anomalies are also observed in the anisotropy of the angular distribution of the fragments in the ^{235}U(d, pf) reaction[66] and in the fission of ^{235}U by p neutrons.[69] It is clear that the difficulties in describing sub-barrier fission are typical for even–even nuclei produced from odd nuclei with high spin of the ground state.

It is difficult to explain these facts by specific fea-

tures of the mechanism of the reactions leading to fission. The effect indicates, rather, that the excited nuclei are "conservative" with respect to changing the internal angular momentum "stored" in the form of the target nucleus's spin in the process of exchange between the collective and nucleon degrees of freedom.[70]

3. EXPERIMENTAL INVESTIGATIONS OF DEEP SUB-BARRIER PHOTOFISSION

The isomer shelf. In discussing the properties of the cross section and the angular anisotropy of photofission, we have deliberately restricted ourselves to the region of energies above 4.5 MeV. First, at lower energies the measurements are hindered by the difficulty of eliminating the background of extraneous fission induced by photoneutrons, this being responsible for the limit achieved in Ref. 37 for the majority of odd nuclei (see Fig. 10). Second, and this is the most important, for nuclei having a sufficiently high threshold in the (n,f) reaction the region of energies that are reached in extended. As a result of measurements made in this region,[71,72] a new effect was discovered in the energy dependence of the yield and the photofission cross section. It became known as the isomer shelf and had a significant influence on the development of experiments in the sub-barrier energy region.

Figure 19b shows the results of the experiment of Bowman *et al.*,[71] in which the effect was observed for the first time in a study of the probability of deep sub-barrier photofission of ^{238}U. The behavior of the photofission cross section at energies below 4.5 MeV is anomalous. In region II it reveals a fairly abrupt slowing down in the rate of its variation compared with the well-studied region I, and as the bottom of the second well, which separates regions I and III, is approached, it changes its behavior even more. The anomaly is associated with delayed fission, i.e., the population and decay of the most long-lived states in the second well—shape isomers. The part played by this process, which makes only a small contribution to the total yield near the fission threshold, increases with decreasing energy and becomes dominant in region II.

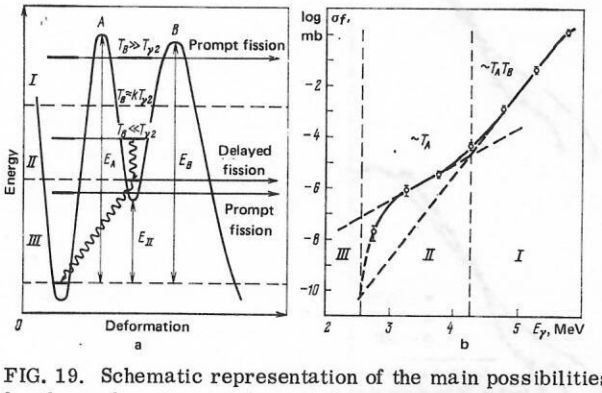

FIG. 19. Schematic representation of the main possibilities for the nucleus to pass through the two-hump barrier for different regions of sub-barrier excitation energies (a) (radiative decay in the first well is not indicated in the figure), and behavior of the photofission cross section in the corresponding energy regions (b).[71]

The contribution of the delayed fission is shown schematically in Fig. 19a. Arriving in the second well during the fission process, the nucleus can divide in two ways: without a change in energy, i.e., promptly, and, having undergone radiative de-excitation, spontaneously from the shape-isomer states at the bottom of the well, i.e., with a delay characterized by the mean lifetime of the nucleus. Since such events were not separated in time in the experiments of Refs. 71 and 72, the observed yield curve describes the total effect of the prompt and delayed fissions. The competition between these mechanisms of fission from the second well is determined by the relationship between two penetrabilities: T_B for passing through the outer hump B and $T_{\gamma 2}$ for radiative de-excitation to the isomer states. As long as $T_B \gg T_{\gamma 2}$, or, more accurately, $T_B \gg kT_{\gamma 2}$, where $k \ll 1$ is the branching coefficient which determines the ratio of the probabilities of spontaneous fission and radiative decay into the first well for the isomer states, prompt fission is predominant in the total yield (region I). In the opposite case ($T_B \ll kT_{\gamma 2}$), the fission process is realized mainly by the population and decay of shape isomers (region II). Since the energy dependence of the prompt-fission cross section is determined by the penetrability of the complete barrier, which is proportional to $T_A T_B$, while the energy dependence of the delayed-fission cross section is determined by the penetrability of the narrower inner hump A, which is $\sim T_A$, it is to be expected that at the point $T_B \approx kT_{\gamma 2}$ the total fission cross section will have a fairly abrupt inflection. In the framework of this qualitative interpretation,[73] and on the basis of Lynn's theoretical description,[74] it is to be expected that the shallow section of the cross section will continue almost to the bottom of the second well, near which there will be a dip even more abrupt than in the steep section $T_B \gg kT_{\gamma 2}$, where prompt fission is predominant.

After the publication of Ref. 71, data indicating similar effects in the yield of the deep sub-barrier photofission of ^{232}Th, ^{238}U, and ^{237}Np were obtained using the microtron of the Institute of Physics Problems.[72]

The photofission cross section in the region of the isomer shelf is negligibly small (less than 10^{-10} b), and this in itself presents serious experimental difficulties for its study. The purity of the employed nuclides plays an important part. An independent problem when one is detecting events with low probability is the study and limitation of the background of extraneous fission, spontaneous and induced by photoneutrons, which can be produced at these low energies of the γ rays in the (γ,n) reaction on deuterium and beryllium nuclei if they are present in the material of the construction and the shield situated in the radiation field. Its importance is revealed by Fig. 20, which shows the experimental data obtained by the authors of the present review on the yield of the (γ,f) reaction in the deep sub-barrier energy region,[75] which, apart from the information on ^{232}Th, ^{238}U, and ^{237}Np (much more complete and of better quality than in the first communication of Ref. 72) and the data on the nucleus ^{236}U (investigated later[76]), contains the results of study of the neutron background. We believe that the abrupt inflection in the yield for ^{235}U, also

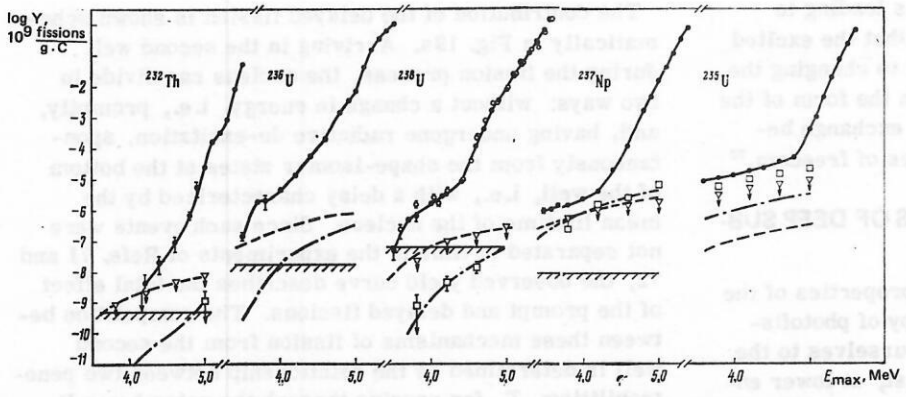

FIG. 20. Results of measurements of the yield $Y(E_{max})$ of the photofission reaction (circles) and also the experimental (triangles) and theoretical (broken curves) estimates of the background of fast-neutron fission events in the reactions Be(γ, n) and D(γ,n) (the rectangles represent the experiment, the chain curves the theory). The broken curve shows the level of the background of spontaneous fission events and fission induced by cosmic rays.

shown in Fig. 20, can be entirely explained by fission induced by neutrons, including neutrons moderated in the walls of the facility. The yield of the (γ, f) reaction for ^{233}U and ^{239}Pu has a similar form.

The final conclusion of Ref. 75 drawn from analysis of the experimental information shown in Fig. 20 is that properties of the energy dependence of the yield associated with the isomer shelf have been definitely established for the nuclei ^{236}U and ^{238}U. For the other two nuclei, the situation is not clear for the following reasons: several series of measurements for ^{232}Th do not reveal a statistically significant effect, and the effect observed for ^{237}Np can be largely explained by the investigated sources of the neutron background.

There are two other published papers, from the United States and Italy, devoted to experimental investigation of the isomer shelf. Bowman *et al.*[77] have given the results of investigations of deep sub-barrier photofission of ^{232}Th and ^{235}U for the same arrangement of the experiment that led to the discovery of the isomer shelf in the yield and cross section of the ^{238}U(γ, f) reaction. A group of Italian physicists[23,78] made detailed measurements of the photofission yield of ^{238}U for E from 3.5 to 6 MeV. A complete sample of the data on this phenomenon for the even–even nuclei investigated theoretically in what follows is shown in Fig. 21.

The reaction yield is the primary information obtained directly in the experiment, but a direct comparison of the results of different authors is usually difficult, since the absolute yields depend on the geometry of the experiment and the characteristics of the bremsstrahlung target. Fortunately, the experimental conditions in our studies[72,75] and those of the Italian group[23,78] were almost completely identical and did not differ strongly from the arrangement of the experiments of Bowman *et al.*[71,77] This can be seen (see Fig. 21) by comparing the original values of the yield with the values calculated for the conditions of our experiments

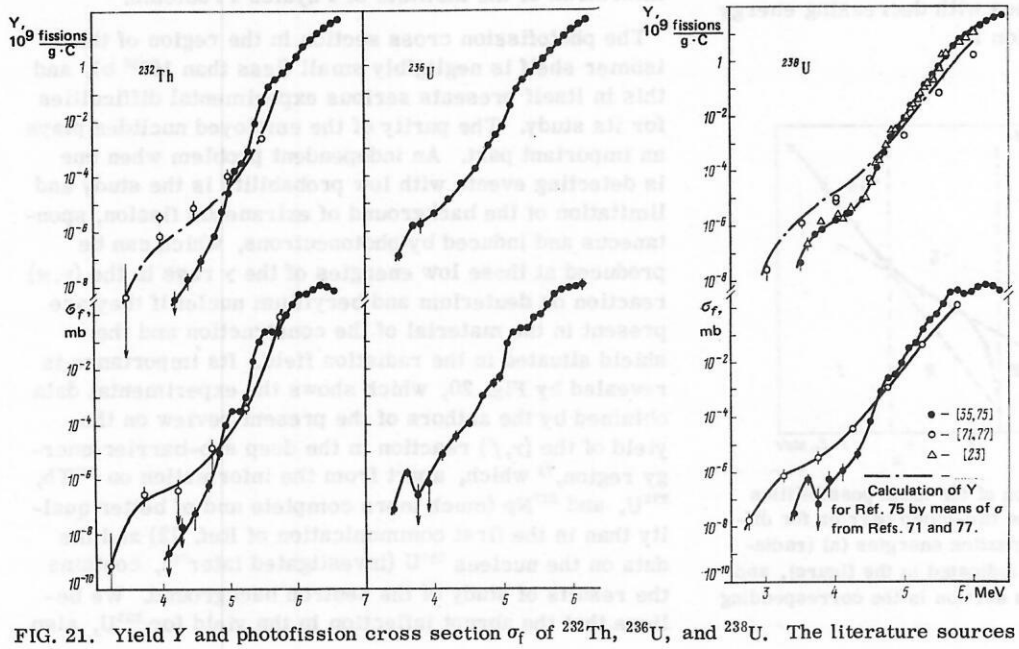

FIG. 21. Yield Y and photofission cross section σ_f of ^{232}Th, ^{236}U, and ^{238}U. The literature sources are given in square brackets.

using the cross sections from Refs. 71 and 77. Note that in our measurements and those of the Italian group the electron source was a microtron, while Bowman *et al.* used an electrostatic accelerator and a linear accelerator.

Despite the similar arrangement of the experiments, a contradictory situation is obtained. The results of our experiments for ^{238}U agree excellently with the data of the Italian group, but for both nuclei (especially for ^{232}Th) there is strong disagreement with the results of the American studies. In the shallow part of the yield, the data disagree by an order of magnitude for ^{238}U and by two orders of magnitude for ^{232}Th. The abrupt dip in the yield in the low-energy section of the shelf is observed for ^{238}U at $E \approx 3.5$ MeV in our data and the Italian data, but in the data of Bowman *et al.* it is observed at least 0.5 MeV lower. The yield curve for ^{232}Th at low energies (at or less than 4.6 MeV) is in our experiments so much steeper than in the American ones that the very existence of the isomer shelf becomes doubtful in this case (for more details, see Ref. 75). The agreement of the results for ^{238}U in the experiments of our group and the Italian group, and also the nature of the discrepancies in Fig. 21—the systematically higher yields in the experiments of Bowman *et al.*[71,77]—cast doubt on the results of the American group in the region of the isomer shelf, although the reaons for the discrepancies are as yet obscure.

A very important result of the more detailed measurements of the yield for ^{236}U and ^{238}U obtained using the microtron of the Institute of Physics Problems was the establishment for both nuclei of a resonance structure of the photofission cross section in the region of the isomer shelf (see Fig. 21). This experimental fact served as a justification for rejecting the theoretical interpretation of the isomer shelf proposed by Bowman.[73] The behavior of the photofission yield at the lowest energies, which indicates a strong resonance in the cross section, is completely confirmed for ^{238}U by the Italian group.[23,78]

With regard to the interpretation of the experimental data, we must add the following. In the simplified treatment of Refs. 71 and 73 it was assumed that the extension of the region of the isomer shelf is fairly clearly defined at the lower end by the bottom of the second well of the fission barrier and at the top end by the inflection in the cross-section curve (or yield curve) of the photofission, which occurs at the energies at which the probabilities of the prompt and the delayed fission become equal. More detailed measurements show that the actual picture is different and more complicated. First, the yields of the (γ, f) reaction exhibit a sharp drop not near the bottom of the second well but much higher, about 1 MeV higher. A resonance in the cross sections corresponds to the edge of the step in the yield curve (see Fig. 21). Second, the notion of an upper end of the region of the isomer shelf is strongly idealized, and in the case of ^{236}U an inflection is not observed at all. This indicates, on the one hand, the unreliability of an interpretation which ignores the circumstance that the experimentally observed fission probability is a superposition of contributions of individual fission channels and, on the other hand, the difficulties in studying the effect by means of measurements of integral characteristics alone. The measurements of the angular distribution of the fragments from deep sub-barrier photofission made using the microtron of the Institute of Physics Problems[33,79] made possible a new step in the study of the isomer shelf.

Anisotropy of the angular distribution of fragments and delayed fission. Because the photofission cross section is negligibly small in the region of the isomer shelf, the separation of the events in time on the background of the γ rays, whose number in the beam exceeds by more than 10^{20} times the number of fission events, presents as yet an insuperable difficulty. In this connection, an independent verification of the proposed nature of the isomer shelf acquired great importance. It was the experiment of Ref. 79, which established isotropy of the fragment angular distribution in the ^{238}U(γ, f) reaction in the region of the isomer shelf (Fig. 22); this is expected in accordance with the properties of delayed fission and is in sharp contrast to the strong anisotropy of prompt fission. Indeed, if the deep sub-barrier anomalies in the yield of the (γ, f) reaction are due to the contribution of delayed fission, there must be a significant decrease in the anisotropy of the fragment emission due to the disorientation of the angular momentum of the nucleus when γ rays are emitted in the second well, and also due to the coupling of the angular momentum to the magnetic field of the atom. In addition, if the main contribution to the delayed fission of even–even nuclei results from decay of the shape isomer in the lowest state $J^{\pi} = 0^{+}$, angular anisotropy must be altogether absent.

In the subsequent experiments of Refs. 33 and 76 there was a systematic investigation of the angular anisotropy of the deep sub-barrier photofission of ^{236}U, and the range of previously investigated[18,19] energies for the nuclei ^{238}U and ^{232}Th was also extended. Figure 23,

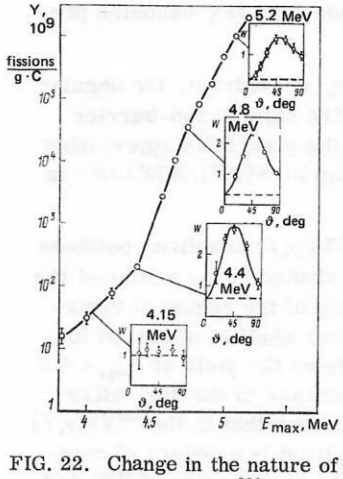

FIG. 22. Change in the nature of the angular distribution $W(\vartheta)$ of the fragments from ^{238}U photofission (in the inserts) with decreasing excitation energy and the approach to the region of the isomer shelf in the yields $Y(E_{max})$. The broken line in the inserts is the isotropic component of the angluar distribution.[79]

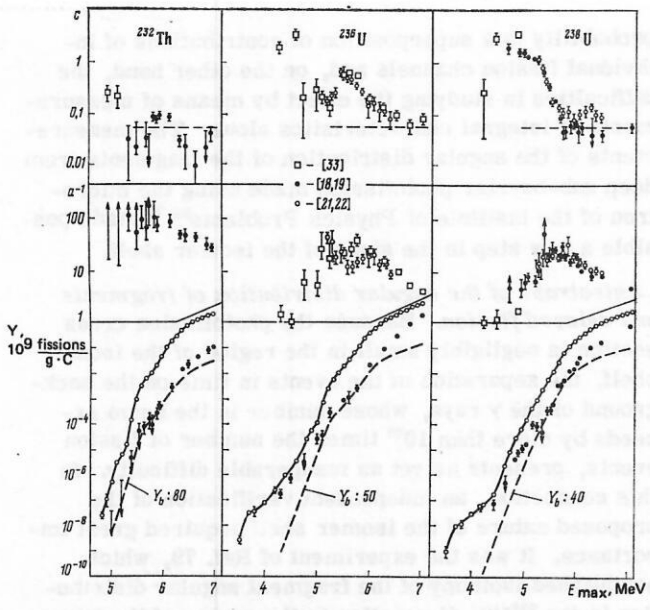

FIG. 23. Dependence of the parameters of the angular distribution of the photofission fragments of ^{232}Th, ^{236}U, and ^{238}U on E_{max}, and also the total photofission yields of the corresponding nuclei (open circles),[37,75] the isotropic component Y_a of the yield (black circles), and the dipole component Y_b, which is made equal to Y_a in the region of the maximum of the anisotropy a^{-1} (broken curves). The broken line in the upper part of the figure shows the asymptotic value of the coefficient $c \approx c/b \approx 0.05$ at energies above the barrier. The literature sources are given in square brackets.

which is taken from Ref. 33, shows the results of the measurements of the angular distribution of the fragments from ^{232}Th, ^{236}U, and ^{238}U at energies $E_{max} \leq 7$ MeV (these measurements were made using the microtron of the Institute of Physics Problems) and also data of similar measurements for the nuclei ^{236}U and ^{238}U in the narrower energy range $E_{max} = 5.2-6.4$ MeV made in Sweden.[22] The following conclusions can be drawn from examination of the experimental data in Figs. 21–23.

1. For both the uranium isotopes, the contribution of the isotropic component rapidly increases as the region of the isomer shelf is approached and, as is shown by the measurements for ^{238}U (see Fig. 21), becomes predominant within the region.

2. In the ^{232}Th(γ,f) reaction, in contrast, the angular anisotropy is large in the entire studied sub-barrier region of energies, in which the yield falls appreciably below the level at which the dip in $W(90°)/W(0°) = a^{-1}$ is observed for ^{238}U and ^{236}U.

3. The probability of the ^{232}Th(γ,f) reaction continues to decrease with virtually no change in the nature of the energy dependence in the whole of the region of variation of $Y(E_{max})$ where the isomer shelf is observed for both the uranium isotopes. From the yield at $E_{max} < 4.8$ MeV, where a pronounced decrease in the derivative dY/dE_{max} was noted, it can be seen that in the ^{232}Th(γ,f) reaction delayed fission is at least two orders of magnitude less probable than in the photofission of ^{236}U and ^{238}U.

4. The results of measurements of the angular distribution of the fragments in the deep sub-barrier energy region have significantly augmented the existing picture of the photofission of even–even nuclei and have emphasized the differences in the behavior of the integral and differential characteristics of the probability of the (γ,f) reaction in the uranium isotopes, on the one hand, and in ^{232}Th, on the other.

The isotropy of the photofission in the region of the isomer shelf agrees with the interpretation of the shelf as an effect due to delayed fission—the decay of an isomer in the second well. On the basis of this experimental fact, we can also understand the reason for the decrease in the angular anisotropy in the sub-barrier photofission of ^{238}U and ^{236}U. This property and the isotropy of the fission in the region of the isomer shelf can be explained naturally from a common point of view as due to an increase in the contribution of delayed fission to the total yield with the increasing probability of radiative de-excitation in the second well compared with the probability of passing through the outer barrier. The same standpoint explains the absence of such an effect in the photofission of ^{232}Th, for which delayed fission is less probable, both on account of the shallower second well and as a consequence of the greater penetrability of the inner barrier A, which facilitates a return to the first well.

A clear picture of the competition between the delayed and the prompt fission can be obtained by means of the angular components of the yield: the isotropic component Y_a and the dipole component Y_b. In Fig. 23, the isotropic component is given in the same units as the total yield, and the dipole component is reduced to make the Y_b curve match the experimental data in the region of the maximum (plateau; see Fig. 5a) of the ratio b/a. It can be seen that for ^{236}U and ^{238}U the curves diverge strongly, but that in the case of ^{232}Th the divergence, explained by the contribution of the delayed fission to Y_a, is absent.

Thus, the observation of the common and opposite properties of the photofission of ^{236}U and ^{238}U on the one hand and ^{232}Th on the other has led to a more complete picture of the relationship between the probabilities of delayed and prompt fission, this picture being in reasonable agreement with what is known about the shape of the barriers of these nuclei. Further, the simultaneous interpretation of the anomaly of the isotropic component of $W(\vartheta)$, which was already noted in the early experiments of Refs. 18 and 19 (see Figs. 5 and 12), and the isomer shelf in the yields has made it possible to combine in a single consistent picture properties such as the angular anisotropy of fission and shape isomerism, which did not appear to be directly related to each other. We note that the idea of a possible connection between these properties was first conjectured by Huizenga.[80] Finally, the measurements of the angular distribution of the fragments also have methodological significance, since the elimination from the total yield of both of its anisotropic components significantly extends the possibilities of studying the isomer-shelf effect. On the background of the much less probable isotropic component, this device is used be-

low in quantitative analysis of the deep sub-barrier photofission of even–even nuclei.

4. THEORETICAL ANALYSIS OF DEEP SUB-BARRIER PHOTOFISSION

The arguments relating to the physical nature of the isomer shelf put forward in the first papers[71-73] and presented at the beginning of the previous section were based on fairly rough estimates of the probability of prompt and delayed fission by means of the hump penetrabilities T_A and T_B. They do not reflect the complicated picture which must obtain in the very sparse region of the state spectrum at the minima of the nuclear deformation potential energy and which is confirmed experimentally. The experimental data in Fig. 21 cover a region of excitation energies that in the second well reaches the edges of the energy gap. At these energies, it is, in describing the fission probability, necessary to take into account complicated aspects of the mechanism such as the coupling between the fission degrees of freedom and the degrees of freedom that do not directly lead to fission and the interactions, responsible for this coupling, between the quantum states within one well and states that belong to different wells. In the considered range of energies, the mean distance between the levels in the wells and the penetrabilities of the humps of the fission barrier change by many orders of magnitude. This circumstance, which governs the change in the nature of these interactions, is the main difficulty in the analysis of experimental data in the deep sub-barrier region, that is, the choice of a theoretical basis for the unified description of real physical situations which change rapidly with the energy.

The probability of near-threshold fission was analyzed earlier by a model of the penetrability of a one-dimensional two-hump barrier in which one assumes complete damping of the vibrational mode (homogeneous distribution over the compound states) in the first well and introduces into the potential an imaginary correction by analogy with the nuclear optical model in order to describe partial damping of that mode in the second well.[44,46] The use of the model is restricted by the condition of there being a fairly large number of compound states within the width of the resonances of the barrier penetrability; this is a condition which is not satisfied in the greater part of the energy range in which we are interested and certainly not in the region of the isomer shelf.

For quantitative interpretation of the isomer shelf, an attempt was made in the first studies[71,73,81] to use the approach developed in the framework of perturbation theory by Lynn[74] and Lynn and Back[82] to describe processes in which only the coupling between compound states in different wells is important. By means of such a model, augmented by the assumption of complete damping of the vibrational mode in both wells, it was possible to expect some kind of an estimate of the nature of the energy dependence of the probabilities of delayed and prompt fission on the average. There could be no talk of an explanation of the resonance structure of the isomer shelf by means of the model.

The approach adopted in the present paper is based on the model of doorway states and was developed recently in Refs. 83 and 84; it has been tested in analysis of the probabilities of prompt and delayed fission in direct reactions.[66,84,85] This approach reflects most fully the specific interaction of the fission and nonfission states, and the perturbation-theory formalism used in it represents a step toward an adequate description of fission in the region of the very sparse spectra in both wells. Another important advantage is the previously absent possibility of a unified description of the probability of sub-barrier fission in the entire experimentally studied energy region.

Description of the fission probability in the model of doorway states. The source of the fission width of an excited state of the compound nucleus is the admixture of the fission mode in its wave function which results from the coupling between fission vibrational modes and the states of nonfission nature which are excited at the initial stage of the reaction. The fission mode is usually associated with β vibrations and the simple collective motions of the nucleus coupled to them—rotations, octupole vibrations, γ vibrations, etc. In the majority of cases, the density of the corresponding states is much lower than the density of the corresponding internal excitation states; thus, the fission states play the part of doorway states for the fission process.

The total Hamiltonian H of the fissioning nucleus can be split into two parts: H_0, for which the doorway states $|A\rangle$ and the nonfission states $|a\rangle$ are eigenstates, and V, which describes the interaction between the states $|A\rangle$ and $|a\rangle$. Then the eigenstate of the compound nucleus ($|\alpha\rangle$) will be a linear superposition of the unperturbed states:

$$|\alpha\rangle = C_{\alpha A}|A\rangle + \sum_a C_{\alpha a}|a\rangle, \tag{28}$$

where $C_{\alpha A}$ and $C_{\alpha a}$ are elements of the matrix which diagonalizes H in the space of the eigenstates of H_0. We are interested in the distribution of the squares of the amplitudes, $C^2_{\alpha A}$, which describe the admixture of the doorway state $|A\rangle$ in the diagonalized states $|\alpha\rangle$; it can be obtained in a simple form by making the following assumptions about V:

$$\langle A|V|A\rangle = \langle a|V|a'\rangle = 0 \quad \text{for all} \quad |a\rangle, |a'\rangle; \tag{29}$$

$$\langle A|V|a\rangle = \langle a|V|A\rangle = V_{Aa} = \text{for every } |a\rangle \tag{30}$$

and about the distance D_a between the states $|a\rangle$: D_a = const. Then[87]

$$C^2_{\alpha A} = \frac{V^2_{Aa}}{(E_\alpha - E_A)^2 + V^2_{Aa} + \pi^2 V^4_{Aa}/D^2_a}. \tag{31}$$

Here, E_α and E_A are the energies of the states $|\alpha\rangle$ and $|A\rangle$, respectively. Frequently, $V^2_{Aa} \ll \pi^2 V^4_{Aa}/D^2_a$, and then the energy distribution of the strength of the doorway state can be expressed in the form of a Lorentzian curve with width $\Gamma_{Aa} = 2\pi V^2_{Aa}/D_a$, which is usually called the damping width of the doorway state:

$$C^2_{\alpha A} \approx \frac{D_a}{2\pi} \frac{\Gamma_{Aa}}{(E - E_A)^2 + \Gamma^2_{Aa}/4}. \tag{32}$$

At a low density of the states $|a\rangle$ or for small V_{Aa}, the situation $\Gamma_{Aa} < D_a$ may be realized. In this case,

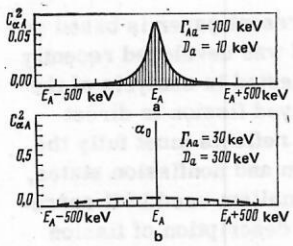

FIG. 24. Examples of the distributions $c^2_{\alpha A}$ of the strength of the doorway state $|A\rangle$ over the compound states $|a\rangle$ for strong (a) and weak (b) coupling.

the doorway state remains a practically pure doorway state, and only a small part of its strength is distributed over the other compound states. The distribution of this residual strength can be obtained in the first order of perturbation theory[74,84]:

$$C^2_{\alpha A} \approx (D_a/2\pi)\,\Gamma_{A\alpha}/(E_\alpha - E_A)^2, \quad E_\alpha \neq E_A. \tag{33}$$

Formally, (33) is equivalent to a Lorentzian distribution with width $\Gamma \approx 2D_a/\pi$, and it can describe the smooth part of the $C^2_{\alpha A}$ distribution for strong and weak damping by a single Lorentzian expression with width

$$\Gamma_A = [\Gamma^2_{A\alpha} + (2D_a/\pi)^2]^{1/2}. \tag{34}$$

The practically pure doorway states $|\alpha_0\rangle$ which remain in the case of weak damping must be taken into account separately. The coefficient $C^2_{\alpha_0 A}$ for such a state can be found by means of the sum rule

$$C^2_{\alpha_0 A} = 1 - \sum_{\alpha \neq \alpha_0} C^2_{\alpha A} \approx 1 - \{[\Gamma^2_A - (2D_a/\pi)^2]^{1/2}/\Gamma_A\}. \tag{35}$$

Examples of the $C^2_{\alpha A}$ distribution for strong and weak damping are shown in Fig. 24.

In the general case, the total width Γ_A of the doorway state is determined not only by the damping width but also by the decay widths of the state $|A\rangle$ (for example, the fission width Γ_{Af} and the fission-related radiative width $\Gamma_{A\gamma}$):

$$\Gamma_A = [\Gamma^2_{A\alpha} + \Gamma^2_{Af} + \Gamma^2_{A\gamma} + (2D_a/\pi)^2]^{1/2}. \tag{36}$$

The picture becomes even more complicated in the two-hump model, since the states of the fissioning nucleus can be divided in the sub-barrier region into two classes of doorway states and two classes of compound states, this depending on whether the maximum of the amplitude of the state wave function corresponds to a deformation of the first (class I) or second (class II) well. Thus, it is now necessary to take into account the coupling of the doorway states to the compound states within each class as well as for different classes.

There are several approaches to the solution of this problem based on different approximations. Back[88] considered the case of the interaction of doorway states of one class—the fission vibrations of class II—with the compound states of both classes. In this case, complete diagonalization of the Hamiltonian gives an exact but rather cumbersome result. In the present paper, we use the less rigorous but simpler and more perspicuous treatment of Refs. 83 and 84. The doorway states of class I ($|A\rangle$) and class II ($|B\rangle$) are diagonalized separately with the compound states of class I ($|a\rangle$) and class II ($|b\rangle$). The resulting compound states $|a'\rangle$ and $|b'\rangle$ belong to the same classes as the unperturbed states $|a\rangle$ and $|b\rangle$, respectively. However, the states $|a'\rangle$ and $|b'\rangle$ are not orthogonal, which is taken into account[83] by the introduction of the widths of their interaction with each other, $\Gamma_{a'b'}$ and $\Gamma_{b'a'}$, this interaction being mediated through their interaction with the doorway states:

$$\Gamma_{a'b'} = \sum_A C^2_{a'A}\Gamma_{Ab} + \sum_B C^2_{a'B}\Gamma_{Bb}; \tag{37}$$

$$\Gamma_{b'a'} = \sum_A C^2_{b'A}\Gamma_{Aa} + \sum_B C^2_{b'B}\Gamma_{Ba}. \tag{38}$$

Here, Γ_{Aa} and Γ_{Bb} are the damping widths of the doorway states $|A\rangle$ and $|B\rangle$ with respect to the compound states within one class; Γ_{Ab} and Γ_{Ba} are the same with respect to the compound states of the other class. It is usually assumed that the interaction between the fission mode and the compound states depends directly on the overlapping of their wave functions in the deformation space. This leads to the relations

$$\Gamma_{Ab} = T_A\Gamma_{Bb}; \quad \Gamma_{Ba} = T_A\Gamma_{Aa}, \tag{39}$$

where T_A is the penetrability of the inner hump A. As in the case of (32), for the squares of the amplitudes in (37) and (38) we can write

$$C^2_{a'A} = (D_a/2\pi)\,\Gamma_{Aa}/[(E - E_A)^2 + \Gamma^2_A/4]; \tag{40}$$
$$C^2_{b'B} = (D_b/2\pi)\,\Gamma_{Bb}/[(E - E_B)^2 + \Gamma^2_B/4]; \tag{41}$$
$$C^2_{a'B} = (D_a/2\pi)\,\Gamma_{Ba}/[(E - E_B)^2 + \Gamma^2_B/4]; \tag{42}$$
$$C^2_{b'A} = (D_b/2\pi)\,\Gamma_{Ab}/[(E - E_A)^2 + \Gamma^2_A/4], \tag{43}$$

where in the total widths of the Lorentzian curves (40)–(43) we have taken into account the damping of the doorway states with respect to the compound states of both classes:

$$\Gamma_A = [(\Gamma_{Aa} + \Gamma_{Ab})^2 + \Gamma^2_{Af} + \Gamma^2_{A\gamma} + (2D_a/\pi)^2]^{1/2}; \tag{44}$$
$$\Gamma_B = [(\Gamma_{Bb} + \Gamma_{Ba})^2 + \Gamma^2_{Bf} + \Gamma^2_{B\gamma} + (2D_b/\pi)^2]^{1/2}. \tag{45}$$

The fission width of the doorway states for the two-hump barrier is

$$\Gamma_{Bf} = (\hbar\omega_{II}/2\pi)\,T_B; \quad \Gamma_{Af} = (\hbar\omega_I/2\pi)\,T_AT_B, \tag{46}$$

where T_B is the penetrability of the outer barrier B; $\hbar\omega_I$ and $\hbar\omega_{II}$ are the curvature parameters of the first and second well, respectively. The compound states $|a'\rangle$ and $|b'\rangle$ will have a fission width due to the coupling of $|a\rangle$ and $|b\rangle$ directly to the doorway states:

$$\Gamma^{dir}_{af} = \sum_A C^2_{aA}\Gamma_{Af} + \sum_B C^2_{aB}\Gamma_{Bf}; \tag{47}$$
$$\Gamma_{bf} = \sum_A C^2_{bA}\Gamma_{Af} + \sum_B C^2_{bB}\Gamma_{Bf}. \tag{48}$$

Here and in what follows, we have for simplicity omitted the prime in the designation of the diagonalized states $|a'\rangle$ and $|b'\rangle$.

The coupling of the compound states with one another [see (37) and (38)] leads to the appearance of an additional fission width of these states. The widths of interest here are those of the compound states of class I, $|a\rangle$, since it is clear that it is these states which are excited in the initial stage of reactions of the type (n,f), (d,pf), (t,pf), and (γ,f) at the energies for which it is

meaningful to divide the states into the two classes. In the calculation of the additional fission width of a state, the compound state $|b\rangle$ with its fission width (48) can be regarded as a doorway state for $|a\rangle$, and the width Γ_{ba} (38) as the damping width of $|b\rangle$ with respect to the states $|a\rangle$, i.e.,

$$\Gamma_{af}^{\text{ind}} = C_{ab}^2\Gamma_{bf} = (D_a/2\pi)\,\Gamma_{ba}\Gamma_{bf}/[(E_a - E_b)^2 + \Gamma_b^2/4]. \quad (49)$$

The total width Γ_b in (49) contains not only the interaction width Γ_{ba} but also the fission width Γ_{bf} and the width of radiative decay of the compound state in the second well: $\Gamma_{b\gamma}$. The expression (49) will also describe the smooth part of the fission width due to the distribution of the residual strength of the state $|b\rangle$ over $|a\rangle$ in the case $\Gamma_{ba} < D_a$, if, as in the case of (34), the effective width $2D_a/\pi$ is included in Γ_b. Thus,

$$\Gamma_b = (\Gamma_{ba}^2 + \Gamma_{bf}^2 + \Gamma_{b\gamma}^2 + 2D_a/\pi)^{1/2}. \quad (50)$$

In the general case, many states $|b\rangle$ may contribute to Γ_{af}^{ind}, and therefore (49) must be summed over all $|b\rangle$. The summation can be readily performed if one assumes equidistance of $|b\rangle$ in the neighborhood of the considered state $|a\rangle$. Then[82]

$$\Gamma_{af}^{\text{ind}} = \Gamma_{ab}\frac{\Gamma_{bf}}{\Gamma_b}\frac{\sinh(\pi\Gamma_b/D_b)}{\cosh(\pi\Gamma_b/D_b) - \cos[2\pi(E_a - E_0)/D_b]} = \Gamma_{ab}\frac{\Gamma_{bf}}{\Gamma_b}f_b, \quad (51)$$

where E_0 is the energy of the $|b\rangle$ level nearest to $|a\rangle$. Thus, we obtain the result known from previous analyses (see, for example, Refs. 82 and 46), namely, the fission width

$$\Gamma_{af} = \sum_A C_{aA}^2\Gamma_{Af} + \sum_B C_{aB}^2\Gamma_{Bf} + \Gamma_{ab}\frac{\Gamma_{bf}}{\Gamma_b}f_b \quad (52)$$

of the class I states consists of a "direct" component, which describes fission from the state $|a\rangle$ directly through the two-hump barrier as a result of coupling to the fission vibrations of the classes I and II, and the "indirect" component, which includes the damping of the vibrations with respect to the compound states of the second well and depends on the structure of the class-II compound states.

Besides prompt fission, the interaction of the compound states $|a\rangle$ and $|b\rangle$ will also lead to the population of the isomer state through radiative de-excitation in the second well:

$$\Gamma_{a\,\text{iso}}^{\text{ind}} = \Gamma_{ab}\,(\Gamma'_{b\gamma}/\Gamma_b)\,f_b. \quad (53)$$

Here, $\Gamma'_{b\gamma}$ is the effective width of radiative decay of the compound states in the second well leading to population of an isomer level with allowance for the competition from the fission channel at each step of the γ cascade.

In the region of excitation energies where $\Gamma_B < D_b$, the class-II doorway state $|B\rangle$ transfers only a very small fraction of its strength to the compound states $|b\rangle$ and $|a\rangle$. The remaining virtually pure doorway state $|b_0\rangle$ leads under the condition $\Gamma_{b_0} < D_a$ to very narrow ($\Gamma \approx 2D_a/\pi$) resonances in Γ_{af} and $\Gamma_{a\,\text{iso}}$:

$$\Gamma_{af}^{b_0} \approx \frac{D_a}{2\pi}\frac{\Gamma_{Ba}\Gamma_{Bf}}{(E-E_{b_0})^2+\Gamma_{b_0}^2/4}\left(1 - \frac{\sqrt{\Gamma_B^2 - (2D_b/\pi)^2}}{\Gamma_B}\right); \quad (54)$$

$$\Gamma_{a\,\text{iso}}^{b_0} \approx \frac{D_a}{2\pi}\frac{\Gamma_{Ba}\Gamma'_{B\gamma}}{(E-E_{b_0})^2+\Gamma_{b_0}^2/4}\left(1 - \frac{\sqrt{\Gamma_B^2 - (2D_b/\pi)^2}}{\Gamma_B}\right), \quad (55)$$

where $\Gamma'_{B\gamma}$ is the effective radiative width for the vibrational states in the second well.

For comparison with experimental results, it is not the relations for the widths that are of interest but those for the probabilities of prompt, P_{af}^{p}, and delayed, P_{af}^{d}, fission, averaged over the interval between the $|b\rangle$ states. We shall not write out in full the cumbersome expressions for $\langle P_{af}^{p}\rangle$ and $\langle P_{af}^{d}\rangle$ but merely note the basic behavior of the average probabilities of prompt and delayed fission in the sub-barrier region.

At excitation energies below the top of the inner hump, the relation $\Gamma_{af} \approx \Gamma_{af}^{\text{ind}}$ is soon satisfied, and at an energy below both humps $\Gamma_b \ll D_b$. Under these conditions,[84]

$$\langle P_{af}^{p}\rangle_b \approx \frac{1}{D_b}\int_{-D_b/2}^{D_b/2}\frac{\Gamma_{af}^{\text{ind}}}{\Gamma_{af}+\Gamma_{a\,\text{iso}}+\Gamma_{a\gamma}}dE \approx \frac{\Gamma_{ab}\Gamma_{bf}}{\Gamma_{a\gamma}\Gamma_b}\frac{1}{\sqrt{1+C}}; \quad (56)$$

$$\langle P_{af}^{d}\rangle_b \approx \frac{1}{D_b}\int_{-D_b/2}^{D_b/2}\frac{k\Gamma_{a\,\text{iso}}^{\text{ind}}}{\Gamma_{af}+\Gamma_{a\,\text{iso}}+\Gamma_{a\gamma}}dE \approx \frac{\Gamma_{ab}k\Gamma'_{b\gamma}}{\Gamma_{a\gamma}\Gamma_b}\frac{1}{\sqrt{1+C}}, \quad (57)$$

where k is the branching coefficient of the decay of the isomer state, and

$$C = \frac{2}{\pi}\frac{D_b}{\Gamma_b}\frac{\Gamma_b + k\Gamma'_{b\gamma}}{\Gamma_b}\frac{\Gamma_{ab}}{\Gamma_{a\gamma}}. \quad (58)$$

It can be seen from Fig. 25, which shows a typical example of the quantities which occur in (56)–(58), that $C \ll 1$ at low energies ($E \lesssim 4.5$ MeV). For this region

$$\langle P_{af}^{p}\rangle_b \approx \Gamma_{ab}\Gamma_{bf}/(\Gamma_{a\gamma}\Gamma_b); \quad (59)$$

$$\langle P_{af}^{d}\rangle_b \approx \Gamma_{ab}k\Gamma'_{b\gamma}/(\Gamma_{a\gamma}\Gamma_b). \quad (60)$$

At such energies, there is usually very weak coupling of the compound states of the first and the second well, so that in accordance with (50) the width Γ_b is approximately equal to $2D_a/\pi$, and it follows from (59) and (60) that a resonance structure must be observed at the same energies in both the prompt and the delayed fission; moreover, in the prompt-fission probability the structure must be sharper (Lorentzian curve of second degree). If in addition to the relation $\Gamma_b \approx 2D_a/\pi$ the condition of weak damping of the fission vibrations in the second well, $\Gamma_b < D_b$, is satisfied, then (59) and

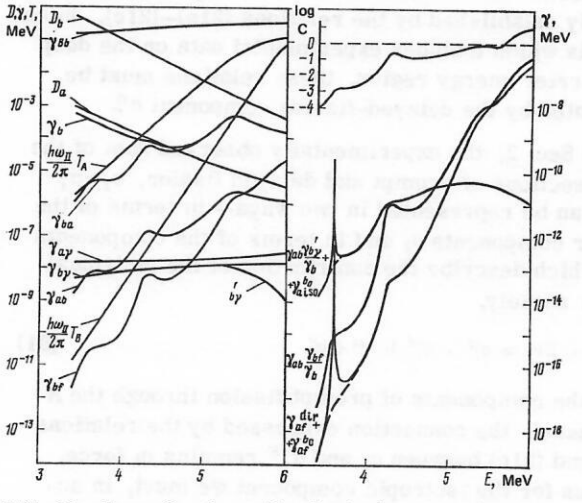

FIG. 25. Example of results of calculation in the doorway-state model of various characteristics for the fission channel J, $K = 2$, 0 of the nucleus ^{236}U and the quantities used in the calculation of the model.[89]

(60) describe only a relatively smooth "substrate," in addition to which narrow resonances, due to the relations (54) and (55), must also be observed.

Since $\Gamma_b \approx 2D_a/\pi$, it can be concluded from the relations (59) and (60) that the probability of prompt fission decreases with the energy much more rapidly (in proportion to $T_A T_B$) than the probability of delayed fission ($\sim T_A$). Therefore, at a certain energy, at which $\Gamma_{bf} \approx k\Gamma'_{b\gamma}$, the probability of delayed fission becomes predominant, and in the curve of the energy dependence of the total probability of prompt and delayed fission this leads to appearance of an inflection due to the transition from the dependence $\sim T_A T_B$ to the weaker $\sim T_A$ (isomer shelf).

Channel analysis of the photofission of ^{236}U *and* ^{238}U. The above approach was used in Ref. 89 for quantitative description of the deep sub-barrier photofission of ^{236}U and ^{238}U. The aim of the theoretical analysis of the results of measurements of the fission probability is usually to recover the barrier parameters and the spectra of the transition states at the saddle points. The difficulties in the way of a unique solution to this problem reside in the rather large number of parameters by means of which the barrier properties can be specified and the complexity of the spectrum of states that can participate in the fission process. As is shown by attempts to analyze the fragment angular distribution in direct reactions,[66] these difficulties cannot be overcome; they are also great in the general case for the (n,f) reaction.[90]

A fundamental advantage of the (γ,f) reaction over other excitation methods is the simplicity of the spectrum of the fission channels which are realized. Because of the strong dependence of the photoabsorption cross section on the multipolarity of the γ rays and of the fissility P_f^λ on E_f^λ, the predominant contribution to the photofission of even–even nuclei near the threshold and at lower energies is made by channels with three $\lambda = (J,K)$, $\pi = (-1)^J$ combinations: (2, 0), (1, 0), (1, 1). If other channels are ignored, the distribution of the photofission cross section over the components can be uniquely established by the relations (21a)–(21c). In an analysis which includes experimental data on the deep sub-barrier energy region, these relations must be augmented by the delayed-fission component σ_f^d.

As in Sec. 2, the experimentally observed sum of the cross sections of prompt and delayed fission, $\sigma_f = \sigma_f^p + \sigma_f^d$, can be represented in two ways— in terms of the angular components σ_i and in terms of the components σ_f^{JK}, which describe the contribution of the individual states; namely,

$$\sigma_f = \Sigma\sigma_i \approx \sigma_f^{20} + \sigma_f^{10} + \sigma_f^{11} + \sigma_f^d. \quad (61)$$

For the components of prompt fission through the $K = 0$ channel, the connection expressed by the relations (21b) and (21c) between σ_i and σ_f^{JK} remains in force, whereas for the isotropic component we must, in accordance with the properties of the fragment angular distribution in the region of the isomer shelf, write

$$\sigma_a = (3/2)\,\sigma_f^{11} + \sigma_f^d, \quad (62)$$

from which we obtain for the components investigated in what follows the cross sections

$$\sigma_f^{20} \approx \sigma_c;\ \ \sigma_f^{10} = \sigma_b + (1/2)\,\sigma_f^{11};\ \ \sigma_f^{11} + (2/3)\,\sigma_f^d = (2/3)\,\sigma_a. \quad (63)$$

Here, to obtain data on the component $\sigma_a(E)$ in the low-energy region we have extrapolated the directly measured dependence $Y_a(E_{max})$ by joining to it at $E_{max} \leq 4$ MeV the data on the total yield, i.e., we have made the assumption that for these energies $Y_a(E_{max}) = Y(E_{max})$.

The calculations of $\sigma_f^{JK}(E)$ and the fitting of the parameters to achieve a description of the experimental data were done under the following assumptions.

1. The Lorentzian dependence with the parameters given in Sec. 2 can be used to describe the photoabsorption cross sections $\sigma_\gamma^{E1}(E)$ and $\sigma_\gamma^{E2}(E)$.

2. In the region of the outer hump, the nucleus is reflection-asymmetric, in connection with which degeneracy, $E_{fB}^{0^+} = E_{fB}^{0^-}$, is assumed for the bands of the channels of positive and negative parity with $K = 0$.

3. When a compound state of class II is formed, there is complete loss of information about the K value with which the nucleus passed through the inner barrier (the model in which K is "forgotten" in the second well). In the calculations of the fission probability for given J, K, π combinations, this assumption is realized by summing over K the widths Γ_{ab} and Γ_{ba} associated with the "transition" through only the inner barrier.

4. For the damping widths of the fission mode a linear dependence on the excitation energy is adopted[74,84]:

$$\Gamma_{Bb}(E) = \Gamma_{Aa}(E - E_{II}) = \alpha + \beta\,(E - E_{II} - 2\Delta_0), \quad (64)$$

where E_{II} is the ground-state energy in the second well, $2\Delta_0$ is the energy gap in the spectrum of the internal excitations, and α and β are coefficients determined directly in the analysis. To estimate the width of the energy gap in the second well, the value $\Delta_0 = 0.6$ MeV is used.

5. To calculate D_a and D_b and the radiative widths, the description of the level density in the model of a superfluid nucleus with phenomenological allowance for the collective and shell effects[91] is used. The level density in the first well is normalized to the known density $\rho_a(B_n)$ of neutron resonances. The difference between the level densities in the first and second wells is taken into account by a simple shift of the excitation energy:

$$\rho_b(E) = \rho_a(E - E_{II}). \quad (65)$$

The γ decay width of the compound states is calculated under the assumption of predominance of E1 transitions, which satisfy the ε_γ^3 rule (ε_γ is the transition energy):

$$\Gamma_\gamma(E) = R\,[\rho(E)]^{-1} \int_0^E \varepsilon_\gamma^3 \rho(E - \varepsilon_\gamma)\,d\varepsilon_\gamma. \quad (66)$$

The constant R was chosen from the condition of normalization of the radiative decay width in the first well to the value in the region of the neutron resonances.

As for the level density, for the radiative width in both wells we take

$$\Gamma_{b\gamma}(E) = \Gamma_{a\gamma}(E - E_{II}). \quad (67)$$

In the calculation of the effective γ decay width in the second well, which results in population of an isomer level,

$$\Gamma'_{b\gamma}(E) \approx \Gamma_{b\gamma}(E)\,\Gamma_{b\gamma}(E - \varepsilon_\gamma)/[\Gamma_{b\gamma}(E - \varepsilon_\gamma) + T_B(E - \varepsilon_\gamma)\,D_b(E - \varepsilon_\gamma)/2\pi] \quad (68)$$

the simplifying assumption is made that all the transitions in the cascade take place with the same, most probable energy $\varepsilon_\gamma \approx 1$ MeV. For the width of the radiative transitions between the collective doorway states in the second well the estimate $\Gamma_{B\gamma} \approx 30$ meV (Ref. 84) is used. The effective width $\Gamma'_{B\gamma}$ is estimated in the same way as $\Gamma'_{b\gamma}$, except that $T_B D_b/2\pi$ in (68) is replaced by $T_b\hbar\omega_{II}/2\pi$, and ε_γ is replaced by the distance between the $|B\rangle$.

In Table I, we give the values of some of the constants used in the analysis: the neutron binding energy B_n,[47] the mean distance between the levels at $E = B_n$ for zero spin, $D(B_n, 0^+)$,[92] the radiative width $\Gamma_\gamma(B_n)$,[92] the ground state in the second well E_{II},[93,94] and the branching coefficient k for isomer decays.[93,94] An example of the energy dependence of the quantities D_a, D_b, $\Gamma_{a\gamma}$, $\Gamma_{b\gamma}$, Γ_{Bb} used in the analysis is given in Fig. 25.

After the assumptions described above, the free parameters which remain in the theoretical description and can be used to fit the calculated curves to the experimental data are the barrier parameters $E_{fA,B}^{K\pi}$ and $\hbar\omega_{A,B}$ and the coefficients α and β, which determine the energy dependence of the damping width (64).

The results of the analysis of the components of the ^{236}U and ^{238}U photofission cross sections are given in Fig. 26, and the parameters of the fission barriers in Table II. The sum of the calculated components is compared with the experimental total fission cross sections in Fig. 27. For the component σ_f^{20}, the calculation was restricted to the region $E \lesssim 6$ MeV, at the boundary of which one must expect $K \neq 0$ channels, which decrease the quadrupole component in $W(\vartheta)$, to begin to play a part. For the dipole components, the calculation was continued to $E_\gamma = 7$ MeV, in connection with which the competition of the (γ, n) processes was taken into account; their thresholds are indicated in Table I and in Fig. 27. Here, the known level schemes of the residual nuclei[95] and the neutron penetrabilities from Ref. 96 were used.

Because of the broad experimentally studied energy range, the barrier parameters $E_{fA}^{K\pi}$, $E_{fB}^{K\pi}$, $\hbar\omega_{A,B}$ can be

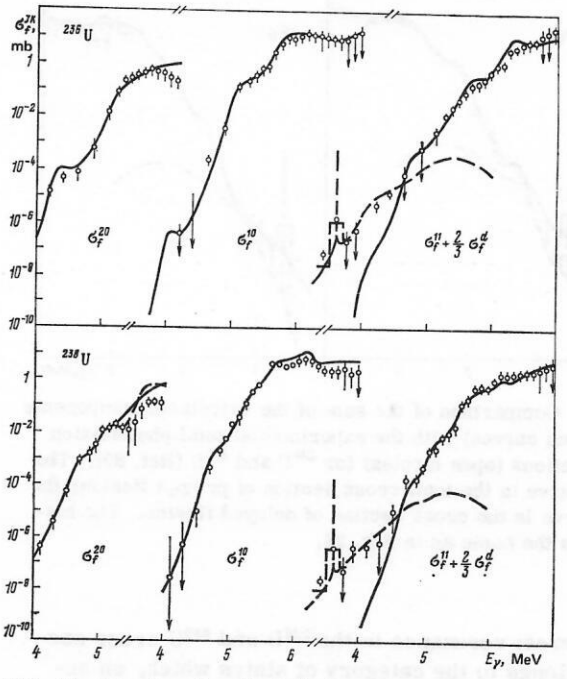

FIG. 26. Results of analysis[89] of the components of the photofission cross section of ^{236}U and ^{238}U. The circles are the cross sections recovered from the measured yields; the continuous curves are the calculation in the doorway-state model of prompt photofission through the lowest channels $(J, K) = (2, 0)$, $(1, 0)$, and $(1, 1)$; the chain curve is the result of calculation of the total contribution of delayed fission from the isomer state populated through the indicated channels (multiplied by 2/3 for comparison with the experimental data; see the text); the histogram shows the calculated delayed-fission cross sections averaged near the narrow resonance over the intervals between the measured points of the yield; the broken curve shows the quadrupole photofission cross section for ^{238}U obtained in Ref. 22.

fixed in fairly narrow intervals:

$$\delta E_{fA}^{0\pi} \approx \pm(0.15 - 0.20)\ \text{MeV}; \quad \delta E_{fB}^{K\pi} \approx \pm(0.10 - 0.15)\ \text{MeV}; \quad \delta\hbar\omega_{A,B} \approx \pm(0.05 - 0.10)\ \text{MeV}, \quad (69)$$

and outside these limits the description of the cross sections deteriorates considerably. For barrier A, the states with $K = 0$ are distinguished, since under the assumption that K is "forgotten" in the second well the sensitivity to the position of the $K = 1$ channel is much lower, as a result of which the error in δE_{fA}^{1-} is appreciably greater, probably by not less than a factor 2, than that of δE_{fA}^{0-}. The resonance structure in the cross sections of both nuclei was described with the parameters $\alpha = 0.15$ MeV and $\beta = 0.1$. In the first well, complete damping was assumed instead of (64), which had virtually no affect on the results of the description.

TABLE I. Values of the constants used in the analysis of Ref. 89.

Nucleus	B_n, MeV (Ref. 47)	$D(B_n, 0^+)$, eV (Ref. 92)	$\Gamma_\gamma(B_n)$, MeV (Ref. 92)	E_{II}, MeV	k
^{236}U	6.546	6.43	42	2.3 [94]	1/6 [94]
^{238}U	6.143	12.4	35	2.56 [93]	1/42 [93]

TABLE II. Parameters of the fission barriers obtained in the fitting of Ref. 89 (MeV).

Nucleus	Barrier A				Barrier B			
	E_f^{0+}	E_f^{0-}	E_f^{1-}	$\hbar\omega$	E_f^{0+}	E_f^{0-}	E_f^{1-}	$\hbar\omega$
^{236}U	5.6	6.45	7.0	1.2	6.0	6.0	6.4	0,7
^{238}U	5.8	6.8	7.0	1.3	6.15	6.15	6.55	0.7

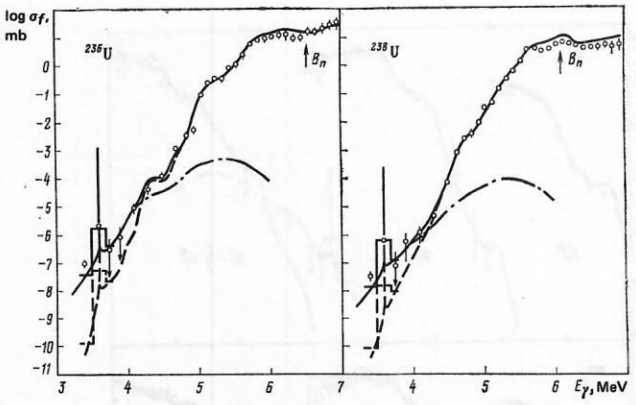

FIG. 27. Comparison of the sum of the calculated components (continuous curves) with the experimental total photofission cross sections (open circles) for ^{236}U and ^{238}U (Ref. 89). The broken curve is the total cross section of prompt fission; the chain curve is the cross section of delayed fission. The histogram is the same as in Fig. 26.

The lowest resonance in the ^{236}U and ^{238}U cross sections belongs to the category of states which, on account of the relation $\Gamma_b \approx D_a \ll D_b$, have widths that are not determined by Eq. (45) but by $D_a \ll \Gamma_{Bb}$. The width is too small compared with the distance $\Delta E_{max} = 0.1$–0.2 MeV between the experimental points in the integral yield $Y(E_{max})$. Since in the recovery of the cross sections from the data on $Y(E_{max})$ we actually use information only about the number of fission events in the interval $E_{max}^{(i+1)} - E_{max}^{(i)}$, the representation of the calculated dependence of the cross sections used in Figs. 26 and 27 in the form of the sections of a histogram which averages the theoretical curve within the step of the measurements will be most adequately adapted to the mathematical evaluation of the experimental data.

Discussion. Resonance structures of the cross sections. By analyzing the resonance structure of the fission cross sections, we can obtain interesting information about the spectrum of the doorway states and the coupling of the fission mode to the other types of motion of the nucleus. Unfortunately, the experiments whose results we have discussed in this paper had different aims and do not contain information sufficiently detailed for such an analysis. The large jump in the energy between the experimental points in the investigations using a bremsstrahlung beam may not only lead to the omission of resonances but also be a source of distortion of the solutions (mainly a smoothing distortion) not only in the interpolation of the original data but also in the recovery of the cross section from the yield. At the present state of the data, these effects are more important than the influence of the energy spread of the electrons in the microtron, which is approximately 30 keV. The difficulties in estimating them, to say nothing of taking them into account, make it impossible to determine the accuracy achieved in the fitting of the parameters in the energy dependence $\Gamma_{Bb}(E - E_{II})$ of the damping width, although it was possible to describe by means of this dependence the resonances at the energies $E - E_{II}$ from 1.5 to 3.2 MeV.

In calculating the curves shown in Figs. 26 and 27, we used the following spectra $E_B^{K^\pi}$ of the doorway states: $E_B^{0^+} = 3.6, 4.3, 5.35$ MeV, $E_B^{0^-} = 4.0, 5.1, 5.85$ MeV, $E_B^{1^-} = 4.7, 5.6, 6.3$ MeV (for ^{236}U) and $E_B^{0^+} = 3.6, 4.7, 5.1$ MeV, $E_B^{0^-} = 4.7, 5.35, 5.7$ MeV, $E_B^{1^-} = 4.7, 4.8, 5.1, 5.55, 5.75$ MeV (for ^{238}U). The greater part of them can be clearly seen directly in the components of the cross sections. Some of the resonances, for example, in the component $\sigma_f^{0^-}$ for the nucleus ^{236}U at $E = 4.0$ MeV, are less clearly expressed, but without allowance for them it is impossible to "maintain" the calculated dependence at the level required by the experiments. In a number of cases, to achieve this it was necessary to take into account two closely spaced states ($E = 4.7$ and 4.8 MeV and 5.55 and 5.75 MeV in $\sigma_f^{1^-}$ for the nucleus ^{238}U) separated by a distance appreciably less than the mean distance between the fission levels, which is about 0.6 MeV. In Ref. 84, the need to introduce a similar "fragmentation" of the doorway states in describing the fissility in direct reactions was also noted.

Note that in the region of the threshold there is a basically reasonable description of the effect of the neutron competition, i.e., the drop in the fissility at $E \gtrsim B_n$, though the observed irregularity is somewhat stronger than in the calculation. The description of the nearby resonance at $E \approx 5.75$ MeV for ^{238}U presented certain difficulties. A way to enhance both effects is known; this is to assume a complicated structure of the outer hump (three-hump barrier),[8] but better data are required for such a particularization.

Parameters of the fission barriers. The results of the present analysis[89] are compared with the ^{236}U and ^{238}U barrier parameters obtained in Refs. 22, 44, 46, 85, and 66 in Fig. 28. Apart from Ref. 22, in which photofission was also used, these are all results obtained by analyzing the fission probability in direct reactions: (d, pf) in Refs. 85, 66, and 44 and (t, pf) in Ref. 46.

There are many reasons for the discrepancies between the data of these studies: the differences between the theoretical models, the parameters, and the assumptions, the different nature of the experimental information as regards both the type of reaction and the energy ranges, and so forth. Some of the discrepancies in the positions $\Delta E_{fA(B)}^{K^\pi} = E_{fA(B)}^{K^\pi} - E_{fA(B)}^{0^+}$ of the channels relative to the ground state are directly related to the initial assumptions about the channel spectrum, since in some papers[22,66] the reflection asymmetry of hump B ($0^- - 0^+$ degeneracy) is taken into account, while in others[44,46,85] it is not. In the first case, as can be seen in Fig. 28, the splitting $\Delta E_{fA}^{0^-}$ is greater, especially for the (γ, f) reaction. In photofission, the contribution of the $0^-(J = 1)$ channel is well separated, whereas in the direct reactions there is no such certainty because of the great number of admissible states.

The ground states $E_{fA(B)}^{0^+}$ and the curvature parameters $\hbar\omega_{A(B)}$ reveal the following tendency, which is due to the differences between the theoretical models of fission. Compared with the penetration model, the doorway-state model leads on the average to higher values of $\hbar\omega_A$ and $\hbar\omega_B$, this decrease in the barrier thickness

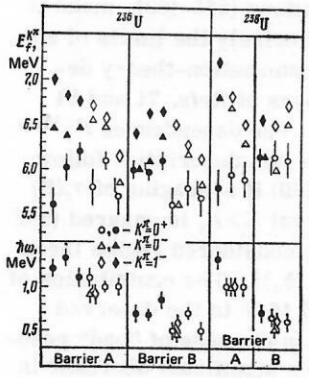

FIG. 28. Comparison of the fission-barrier parameters of ^{236}U and ^{238}U obtained as a result of channel analysis of the experimental data in the following papers (see the points from left to right): Refs. 89, 66, 85, 22, 44, and 46 for ^{236}U and Refs. 89, 22, and 46 for ^{238}U. The black symbols are the results of the analyses in the doorway-state model.

being "compensated" for hump B by the greater height.

There is a striking spread of the $E_{fA}^{0^+}$ values for the nucleus ^{236}U, whereas there is satisfactory agreement for ^{238}U. We note that in the second case only the (γ, f) and (t, pf) reactions were analyzed, and all the larger values in the first case were obtained from analysis of the fissility in the ^{235}U(d, pf) reaction.[44, 85, 66] In Sec. 2, we compared the fissilities $P_f(E)$ for these reactions and found an effect which we interpreted as suppression of the $K = 0$ channels in the fission of nuclei produced from odd target nuclei with high spin (see Fig. 18). The sign of the effect in $P_f(E)$ agrees with the nature of the $E_{fA}^{0^+}$ discrepancies in Fig. 28. We therefore believe that in general the results obtained from reactions with even–even target nuclei warrant preference and, specifically, the lower value of $E_f^{0^+}$ from Ref. 89 is to be preferred among the analyses[66, 85, 89] made using the doorway-state model.

Let us now discuss the influence of the quantum structure of the barrier on the description of delayed fission. In our case, because of the assumption of reflection-asymmetry at the hump B, the splittings $\Delta E_{fA}^{0^-}$ and $\Delta E_{fA}^{1^-}$ are so large that despite the relation $\sigma_\gamma^{E2} \ll \sigma_\gamma^{E1}$ the predominant contribution to the delayed fission in the region of the isomer shelf is made by the quadrupole photoabsorption. The partial contributions to the total cross section of delayed fission of ^{236}U and ^{238}U made by the quadrupole channel $J, K = 2, 0$ and the dipole channels $J, K = 1, 0$ and $1, 1$ (the latter cannot be distinguished in the model in which K is "forgotten") are shown in Fig. 29.

It was not difficult to describe the delayed-fission cross section without recourse to the other quadrupole channels, in particular $J, K = 2, 2$. In Ref. 86, the states with $K^\pi = 2^+$ are accorded an important part because of the assumption made there of axial asymmetry of the nuclear shape at the hump for ^{236}U and the associated degeneracy of the states $K^\pi = 2^+$ and 0^+. It results in a significant increase in the fission probability and, as a consequence, a decrease in the radiative width, used in Ref. 66 as a free parameter, when

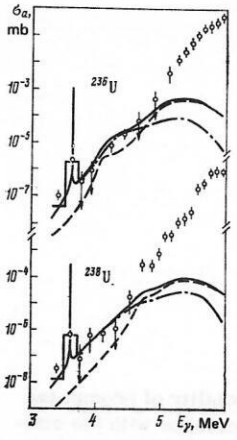

FIG. 29. Partial contributions to the total cross section of delayed fission (continuous curve) of ^{236}U and ^{238}U by the quadrupole channel J, $K = 2$, 0 (chain curve) and the dipole channels J, $K = 1$, 0 and 1, 1 (broken curve).[89] The histogram has the same meaning as in Fig. 26; the circles show the isotropic component σ_a of the photofission cross section.

the experimental data are fitted. However, this assumption is not necessary, since the calculations of Ref. 97 show that the gain in the potential energy at the inner hump resulting from inclusion of the γ deformation, which reaches 1.5–2 MeV in the region of Cm–Fm, decreases rapidly with decreasing number of nucleons and is only about 0.3 MeV for ^{236}U.

We note also that in Ref. 66 a simultaneous analysis of the fission probability in direct reactions and in the (γ, f) reaction for several even–even nuclei, including ^{236}U, was attempted. Even for the yields $Y(E_{max})$ and $Y_i(E_{max})$ the obtained description is much less accurate than in Figs. 26 and 27, which is no surprise in the light of the significant differences between Refs. 66 and 89 (as regards both the initial information and the assumptions used in the analyses). Fundamental in our view are the differences between the fissilities in the (d, pf) and (γ, f) reactions associated with the nucleon composition of the target nuclei and in the assumptions of axial asymmetry of the fissioning nuclei when they pass through the inner barrier.

On a simplification of the theoretical description. The isomer shelf has attracted much interest, both as a new subject of investigation and as a source of information about the structure of the fission barrier. In many of the papers devoted to this question (not only the early papers of Refs. 71 and 81 but also the latest ones of Refs. 98 and 99) the theoretical models used to describe the experimental data have a limited applicability and do not adequately reflect the physical picture which obtains at deep subbarrier excitation energies. To discuss the inaccuracies which result from such simplifications, we have attempted to systematize and compare the various theoretical models of sub-barrier fission.

We distinguish two characteristic cases determined by the relationship between the decay width Γ_b of the compound states in the second well and the mean distance D_a between the analogous states in the first well,

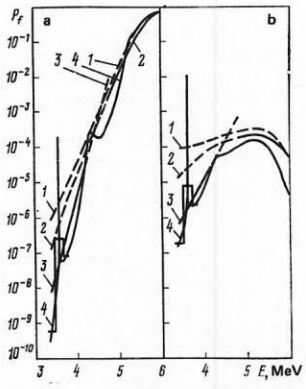

FIG. 30. Energy dependence of the probability of prompt (a) and delayed (b) fission calculated in accordance with the statistical model (1), the two-hump barrier penetrability model (2), perturbation theory (3), and the doorway-state model (4). The broken curves show the same curves beyond the limits of applicability of the corresponding models; the histogram is the result of averaging curve 4 in the region of the narrow resonance. The same parameters as in the analysis of the quadrupole photofission of ^{236}U in Ref. 89 were used.

namely $D_a \ll \Gamma_b$ and $D_a \gtrsim \Gamma_b$; these correspond to different approaches to the theoretical description: the two-hump barrier penetrability model[82] and the model in which the coupling between the compound states of the first and the second well is described by perturbation theory.[74] Differences between these approaches are even manifested in the simplest approximation of complete damping (uniform distribution of the vibrational mode over the compound states); they are illustrated by Fig. 30, which shows the results of calculations of the probability of prompt (a) and delayed (b) fission by the two models, and also the statistical model, whose region of applicability extends downward from the section of near-threshold energies least among the three models. The calculations were made for a barrier with parameters obtained from the channel analysis of the ^{238}U(γ, f) reaction.[89]

The energy ranges in which the above models are applicable do not overlap, and since the intermediate region is small because of the rapid rate of change of the ratio Γ_b / D_a, extrapolation of the relations beyond their limits of applicability may lead to appreciable errors. For comparison, in Fig. 30 we give the results of calculations in the doorway-state model, which ensures a description in a unified approach in the entire considered energy range.

Fundamentally new in the doorway-state model is the possibility of describing the fission probability when the width of the vibrational levels becomes less than the average distance between the compound states in the second well. In this case, the vibrational strength is concentrated on one or two such states, and this results in the realization of virtually pure vibrational resonances $|b_0\rangle$ (very weak damping). The region of the isomer shelf corresponds to the conditions of formation of such resonances, and one of them is manifested in the ^{236}U and ^{238}U photofission cross sections ($E \approx 3.6$ MeV).

The results obtained in the framework of the doorway-state model, namely, the relations (56)–(60), make it possible to determine more precisely the limits of applicability of the simplified perturbation-theory description used in the first papers of Refs. 71 and 81 and shown in Figs. 19 and 30. The dependences $P_f \sim T_A T_B$ and $P_f^d \sim T_A$ expected in this description follow approximately from (59) and (60) if averaging of $\sigma_f(E)$ over a sufficiently large interval $E > D_b$ is ensured (and under the condition that in the considered region there are no purely doorway states $|b_0\rangle$). The contribution of the state of this kind at $E \approx 3.6$ MeV to the observed yield (or to the cross section in the case of "bad" resolution, as in Ref. 71) leads to a significant decrease in the rate of change of dY/dE_{max} in the region of the isomer shelf compared with the estimate $P_f^d \sim T_A$, and in an analysis in which this circumstance is ignored it leads to a distortion of the barrier shape (see Fig. 3 in Ref. 71). Additional inaccuracies in Refs. 71 and 77 arise from the overestimated cross section in the region of the shelf (see Fig. 21), to which attention is drawn in Ref. 100.

Above, we have discussed the analysis made by Bowman's group of the data which they obtained in the ^{238}U(γ, f) reaction.[71] Let us also consider the example of the substantial simplification in the description of deep sub-barrier photofission of ^{232}Th proposed in Ref. 98 by Bhandari. In a wide range of energies, as far as 3.0 MeV, he uses the description in the two-hump barrier penetrability model, despite the fact that for the fission-barrier parameters used in Ref. 98 the range of sub-barrier energies in the second well from the top of the inner hump at $E_{fA} = 3.6$ MeV to the isomer state at $E_i = 2.9$ MeV is only 0.7 MeV, and this is significantly less than the width of the energy gap in the spectrum of the internal excitations of the nucleus. The use of the two-hump barrier penetrability model in this region is completely unjustified, and the doorway-state model (or perturbation theory for the averaged picture) corresponds much more closely to the physical situation. As can be seen from Fig. 30, the two-hump barrier penetrability model calculations in the region of the isomer shelf strongly overestimate the probabilities of prompt and delayed fission compared with the perturbation-theory calculations and even more than for the doorway-state model. Thus, by means of an inadequate reality and an approach which clearly overestimates the delayed-fission probability, Bhandari succeeded in describing the experimental data of Ref. 77—also evidently giving values much too high. Similar comments apply to Ref. 99, in which an attempt is made to use the two-hump barrier penetrability model to describe ^{238}U photofission data in a wide range of subbarrier energies down to the bottom of the second well.

Finally, we consider the question of the characteristic "points," which determine the extension of the isomer shelf, above all the inflection in the energy dependence of the photofission probability, whose position is determined in the simplified description by the equation $T_B = kT_{\gamma 2}$. We have already noted that in the ^{236}U(γ, f) reaction there is no inflection in the total yields, and nor is there one in the isotropic component and the corresponding cross sections. The information presented in

Figs. 26 and 29 shows that the disappearance of the inflection in this case is due to the resonance in the quadrupole component at $E_\gamma = 4.3$ MeV, which happens to lie in the region in which the inflection is manifested in the $^{238}U(\gamma,f)$ reaction. From the same data it can also be concluded that for ^{238}U the effect is, in contrast, emphasized by the higher positions of the resonances in all three components. Obviously, the use of ideas about the "inflection" and the relation given above to estimate the parameters of the outer hump B or the coefficient k (see Refs. 98 and 101) requires care.

We mention finally that the name of the effect—isomer shelf— is somewhat unfortunate (bearing in mind the precise meaning of the English word "shelf"), since even in the most favorable case (^{238}U) the dependence corresponding to it is satisfied only in yields or cross sections with poor energy resolution. The actual picture in this region of energies, which corresponds to a spectrum with a very low density of states near the bottom of the second well, is much richer and more complicated, and the actual picture, and not the effect of its averaging, is of greater interest in the study of deep sub-barrier fission. However the development of these experiments presents difficulties, since the possibilities of the existing sources of monoenergetic electrons for progressing further into the sub-barrier region are almost exhausted.

CONCLUSIONS

The main aim of this review has been to demonstrate the importance and potential of the (γ,f) reaction for the experimental study of the fission mechanism of heavy nuclei. Our attention has been concentrated on the excitation functions and the angular distribution of near-threshold and sub-barrier fission of even–even nuclei. These are the aspects of the fission process, i.e., the excitation regions, and the subjects of investigation for which the quantum properties of the fissioning nuclei are most important and for which the remarkable simplicity of the (γ,f) reaction kinematics can be most fully exploited. We have restricted ourselves to the characteristics that determine the fission probability "in the large," integrally, without particularization of the numerous modes, i.e., the parameters of the paired fragments. The theoretical ideas concerning the integral (in the indicated sense) quantities are much better developed and are directly related to the properties in which we are interested, namely, the shape of the barrier, the discrete nature of the spectrum, the quantum numbers of the transition states and the quasitationary states, and so forth. At the same time, there are theoretical arguments[9,10,102] which make it possible to establish important connections between the asymmetry of the fission and the structure of the barrier, but because of the inadequacy of the experimental information[103] we have not considered this interesting question. It must also be recognized that in giving a definite direction to the review we have necessarily prejudiced the completeness of the presentation and the systematization of the experimental material, and this even in the energy region with which we have been concerned.

Most of the methods of exciting nuclei, including the practically important reaction (n,f), lead to a fairly large set of accessible fission channels, and experimentally one observes the total effect of their contributions. The (γ,f) reaction is a delicate tool that (particularly for even–even nuclei) enables one to separate a small group of the most characteristic channels from this obscure picture; this is its advantage in the experimental investigation of the properties of the probability of induced fission. As an example we may mention the experiments aimed at the direct verification of Bohr's hypothesis of fission channels.

The simplicity of the photofission kinematics has acquired particular significance during the last decade, in which the idea of a two-hump shape of the fission barrier of heavy nuclei has become firmer. The two-hump model has successfully explained a large number of "strange" experimental facts, including, as we have shown in the review, some in the case of the (γ,f) reaction. For example, the observed dependence of the ratios b/a and c/b on the excitation energy and on the nucleon composition of the nucleus is one of the few dependences in which properties of the two-hump barrier such as the ratio of the heights of the humps and the differences in the spectra of the associated transition states are very clearly manifested. The investigations of induced fission made during recent years by means of other excitation methods, above all in direct reactions, also produce a favorable "background" for photofission, revealing an extremely complicated picture (especially in the sub-barrier energy region), for which a satisfactory description has not hitherto been obtained.[66] The results of the channel analysis of the (γ,f) reaction presented in the review are a convincing contrast to this situation.

The possibilities of the (γ,f) reaction are far from exhausted. Even in the existing formulation of the experiments, which are still far from achieving the detail in the measurements required by the theoretical description, only two or three nuclei have been studied, the experimental data for them being relatively suitable for extensive analysis. At the present stage, it is important to extend the number of studied nuclei with appreciable particularization of the energy dependence of the integral and differential cross sections. Of great interest is a new field of very difficult investigations—the physics of induced fission near the bottom of the second well. If important progress is to be made here, we require sources of monoenergetic electrons in the milliampere range. We are still far from solving the problem considered here of the influence of the barrier structure on the fission asymmetry, to which the (γ,f) reaction could make a more significant contribution. Comprehensive investigations into the fission of the same compound nuclei produced in different ways, above all by photo- and electroexcitation and in direct reactions, have great promise.

[1]V. M. Strutinskiĭ, Preprint 1108 [in Russian], I. V. Kurchatov Institute of Atomic Energy, Moscow (1966).
[2]V. M. Strutinsky, Nucl. Phys. **A95**, 420 (1967); **A112**, 1

(1968).
[3]V. M. Strutinsky and S. Bjornholm, in: Proc. Dubna Symposium on Nuclear Structure, IAEA, Vienna (1968), p. 431.
[4]S. Bjornholm and V. M. Strutinsky, Nucl. Phys. **A136**, 1 (1969).
[5]V. M. Strutinsky and H. C. Pauli, in: Proc. IAEA Symposium on the Physics and Chemistry of Fission, IAEA, Vienna (1969), p. 155.
[6]N. Bohr and J. A. Wheeler, Phys. Rev. **56**, 426 (1939).
[7]Ya. I. Frenkel', Zh. Eksp. Teor. Fiz. **9**, 641 (1939).
[8]P. Möller and J. R. Nix, in: Proc. IAEA Symposium on the Physics and Chemistry of Fission, Vol. 1, IAEA, Vienna (1974), p. 103.
[9]P. Möller and S. G. Nilsson, Phys. Lett. **B31**, 283 (1970).
[10]V. V. Pashkevich, Nucl. Phys. **A169**, 275 (1971).
[11]E. J. Winhold, P. T. Demos, and I. Halpern, Phys. Rev. **85**, 728 (1952); **87**, 1139 (1952).
[12]V. P. Perelygin, S. P. Tret'yakova, and I. Zvara, Prib. Tekh. Eksp. No. 4, 78 (1964).
[13]S. P. Kapitsa, V. P. Bykov, and V. N. Melekhin, Zh. Eksp. Teor. Fiz. **41**, 368 (1961) [Sov. Phys. JETP **14**, 266 (1962)].
[14]S. P. Kapitsa, V. N. Melekhin, B. D. Zakirov, *et al.*, Prib. Tekh. Eksp. No. 1, 13 (1969).
[15]L. Katz, A. E. Baerg, and F. Brown, in: Proc. Second Intern. Conf. on the Peaceful Uses of Atomic Energy, Vol. 15, Geneva (1958), p. 188.
[16]A. S. Soldatov, G. N. Smirenkin, S. P. Kapitza, and Yu. M. Tsipenyuk, Phys. Lett. **14**, 217 (1965).
[17]N. S. Rabotnov, G. N. Smirenkin, A. S. Soldatov, *et al.*, in: Proc. Intern. Conf. on the Physics and Chemistry of Fission, Vol. 1, IAEA, Vienna (1965), p. 135.
[18]N. S. Rabotnov, G. N. Smirenkin, A.S. Soldatov, *et al.*, Yad. Fiz. **11**, 508 (1970) [Sov. J. Nucl. Phys. **11**, 285 (1970)].
[19]A. B. Ignatyuk, N. S. Rabotnov, G. N. Smirenkin, *et al.*, Zh. Eksp. Teor. Fiz. **61**, 1284 (1971) [Sov. Phys. JETP **34**, 684 (1972)].
[20]E. A. Zhagrov, Yu. A. Nemilov, and Yu. A. Selitskiĭ, Yad. Fiz. **7**, 264 (1968) [Sov. J. Nucl. Phys. **7**, 183 (1968)].
[21]A. Alm and L. J. Lindgren, Nucl. Phys. **A271**, 1 (1976).
[22]L. J. Lindgren, A. Alm, and A. Sandell, Nucl. Phys. **A298**, 43 (1978).
[23]R. Alba, G. Bellia, L. Calabretta, *et al.*, in: Proc. Intern. Symposium on the Physics and Chemistry of Fission, Vol. 1, IAEA, Vienna (1980), p. 61.
[24]A. Bohr, in: Proc. Intern. Conf. on Peaceful Uses of Atomic Energy, Geneva, 1955, United Nations, New York (1956), p. 151.
[25]J. J. Griffin, Phys. Rev. **116**, 107 (1959).
[26]V. M. Strutinskiĭ, Zh. Eksp. Teor. Fiz. **30**, 606 (1956) [Sov. Phys. JETP **3**, 638 (1956)].
[27]J. R. Huizenga and R. Vandenbosch, in: Yadernye reaktsii (Nuclear Reactions, Russian translation], Vol. 1, Atomizdat, Moscow (1962), p. 51.
[28]A. Bohr and B. R. Mottelson, Nuclear Structure, Vol. 2, Benjamin, Reading, Mass. (1975) (Russian translation published by Mir, Moscow (1977), p. 118).
[29]V. E. Zhuchko, Yu. B. Ostapenko, G. N. Smirenkin, *et al.*, Yad. Fiz. **27**, 1420 (1978) [Sov. J. Nucl. Phys. **27**, 746 (1978)].
[30]N. S. Rabotnov, G. N. Smirenkin, A. S. Soldatov, *et al.*, Nucl. Phys. **77**, 92 (1966).
[31]A. S. Soldatov, Yu. M. Tsipenyuk, and G. N. Smirenkin, Yad. Fiz. **11**, 992 (1970) [Sov. J. Nucl. Phys. **11**, 552 (1970)].
[32]N. S. Rabotnov, A. S. Soldatov, G. N. Smirenkin, *et al.*, Phys. Lett. **B26**, 218 (1968).
[33]V. E. Zhuchko, Yu. B. Ostapenko, G. N. Smirenkin, *et al.*, Yad. Fiz. **30**, 634 (1979) [Sov. J. Nucl. Phys. **30**, 326 (1979)].
[34]R. Vandenbosch, Phys. Lett. **B45**, 207 (1973).
[35]A. Gavron, H. C. Britt, and A. Wilhelmy, Phys. Rev. C **13**, 2577 (1976).
[36]V. E. Zhuchko, S. P. Kapitsa, Yu. B. Ostapenko, *et al.*, Pis'ma Zh. Eksp. Teor. Fiz. **26**, 718 (1977) [JETP Lett. **26**, 553 (1977)].
[37]V. E. Zhuchko, Yu. B. Ostapenko, and G. N. Smirenkin, Yad. Fiz. **28**, 1170 (1978) [Sov. J. Nucl. Phys. **28**, 602 (1978)].
[38]V. E. Zhuchko, Yu. B. Ostapenko, A. S. Soldatov, *et al.*, Nucl. Instrum. Methods **136**, 373 (1976).
[39]M. Z. Tarasko, Preprint No. 156 [in Russian], Physics and Power Institute, Obninsk (1969).
[40]M. V. Yester, R. A. Anderl, and R. C. Morrisson, Nucl. Phys. **A206**, 596 (1973); **A212**, 22 (1973).
[41]J. T. Caldwell, E. J. Dowdy, R. Berman, *et al.*, Report LA-UR 76-1615 (1976); Phys. Rev. C **21**, 1215 (1980).
[42]A. M. Khan and J. W. Knowles, Nucl. Phys. **A179**, 333 (1972).
[43]P. A. Dickey and J. D. Axel, Phys. Rev. Lett. **35**, 501 (1975).
[44]B. B. Back, J. P. Bondorf, G. A. Otroschenko, *et al.*, Nucl. Phys. **A165**, 449 (1971).
[45]B. B. Back, H. C. Britt, O. Hansen, *et al.*, Phys. Rev. C **10**, 1948 (1974).
[46]B. B. Back, O. Hansen, H. C. Britt, *et al.*, Phys. Rev. C **9**, 1924 (1974).
[47]V. A. Kravtsov, Massy atomov i énergii svyazi yader (Masses of Atoms and Binding Energies of Nuclei), Atomizdat, Moscow (1974).
[48]B. Forkman and S. A. E. Johansson, Nucl. Phys. **20**, 136 (1960).
[49]A. Manfredini, L. Fiore, C. Ramorino, *et al.*, Nucl. Phys. **A123**, 664 (1969).
[50]J. W. Knowles, A. M. Khan, and W. G. Cross, Izv. Akad. Nauk SSSR, Ser. Fiz. **34**, 1627 (1970).
[51]E. J. Dowdy and T. L. Krysinski, Nucl. Phys. **A175**, 501 (1971).
[52]P. Axel, Phys. Rev. **126**, 671 (1962).
[53]G. M. Gurevich, L. E. Lazareva, V. M. Mazur, *et al.*, Nucl. Phys. **A273**, 326 (1976).
[54]A. Veyssiere, H. Beil, R. Bergere, *et al.*, Nucl. Phys. **A199**, 45 (1973).
[55]G. R. Satchler, Phys. Rep. **C14**, 99 (1974).
[56]I. N. Borzov and S. P. Kamerdzhiev, Preprint No. 580 [in Russian], Physics and Power Institute, Obninsk (1975).
[57]J. D. T. Arruda Neto, S. B. Herdade, B. S. Bhandari, *et al.*, Phys. Rev. C **18**, 863 (1978).
[58]E. Wolynec, M. N. Martins, and G. Moscati, Phys. Rev. Lett. **37**, 585 (1976).
[59]W. A. Houk, R. W. Moore, F. R. Buskirk, *et al.*, cited in Ref. 57, Table II, p. 869.
[60]W. W. Gargaro and D. S. Onley, Phys. Rev. C **4**, 1032 (1971).
[61]J. R. Huizenga and H. C. Britt, in: Proc. Intern. Conf. on Photonulcear Reactions and Applications, Asilomar (1973), p. 833.
[62]H. C. Britt, in: Ref. 23, p. 3.
[63]V. M. Gorbachev, Yu. S. Zamyatnin, and A. A. Lbov, Vzaimodeĭstvie izluchenii yadrami tyazhelykh élementov i delenie yader (Interaction of Radiations with the Nuclei of Heavy Elements and Fission), Atomizdat, Moscow (1976), p. 54.
[64]O. Y. Mafra, S. Kuniyoshi, and J. Goldemberg, Nucl. Phys. **A186**, 110 (1972).
[65]J. W. Knowles and O. Y. Mafra, in: Ref. 61, p. 647.
[66]M. Just, U. Goerlach, D. Habs, *et al.*, in: Ref. 23, p. 71.
[67]N. J. Pattenden and H. Postma, Nucl. Phys. **A167**, 225 (1971).
[68]R. Kuiken, N. J. Pattenden, and H. Postma, Nucl. Phys. **A190**, 401 (1972).
[69]N. N. Gonin, V. K. Goryunov, J. K. Kozlovskiĭ, *et al.*, Yad. Fiz. **22**, 692 (1975) [Sov. J. Nucl. Phys. **22**, 358 (1975)].
[70]Yu. B. Ostapenko and G. N. Smirenkin, in: Neĭtronnaya fizika (Neutron Physics), Part 3, TsNIIatominform, Moscow (1980), p. 73.
[71]C. D. Bowman, I. G. Schröder, C. E. Dick, *et al.*, Phys. Rev. C. **12**, 863 (1975).
[72]V. E. Zhuchko, A. V. Ignatyuk, Yu. B. Ostapenko, *et al.*,

Pis'ma Zh. Eksp. Teor. Fiz. **22**, 255 (1975) [JETP Lett. **22**, 118 (1975)].
[73]C. D. Bowman, Phys. Rev. C **12**, 856 (1975).
[74]J. E. Lynn, UKAEA Report AERE-R5891, Harwell (1968); in: Ref. 5, p. 249.
[75]V. E. Zhuchko, Yu. B. Ostapenko, G. N. Smirenkin, *et al.*, Yad. Fiz. **28**, 1185 (1978) [Sov. J. Nucl. Phys. **28**, 611 (1978)].
[76]V. E. Zhuchko, A. V. Ignatyuk, Yu. B. Ostapenko, *et al.*, Phys. Lett. **B68**, 323 (1977).
[77]C. D. Bowman, I. G. Schröder, K. C. Duvall, *et al.*, Phys. Rev. C **17**, 1086 (1978).
[78]G. Bellia, Z. Del Zoppo, E. Migneco, *et al.*, Phys. Rev. C **20**, 1059 (1979).
[79]V. E. Zhuchko, A. V. Ignatyuk, Yu. B. Ostapenko, *et al.*, Pis'ma Zh. Eksp. Teor. **24**, 309 (1976) [JETP Lett. **24**, 277 (1976)].
[80]J. R. Huizenga, in: Ref. 5, p. 436.
[81]V. E. Zhuchko, Yu. M. Tsipenyuk, A. V. Ignatyuk, *et al.*, in: Neĭtronnaya fizika (Neutron Physics), Part 3, TsNIIatominform, Moscow (1977), p. 21.
[82]J. E. Lynn and B. B. Back, J. Phys. A **7**, 395 (1974).
[83]P. D. Goldstone and P. Paul, Phys. Rev. C **18**, 1733 (1978).
[84]U. Goerlach, D. Habs, M. Just, *et al.*, Z. Phys. **A287**, 171 (1978).
[85]P. D. Goldstone, F. Hopkins, R. E. Malmin, *et al.*, Phys. Rev. C **18**, 1706 (1978).
[86]L. Wilets, Theories of Nuclear Fission, Clarendon Press, Oxford (1964) [Russian translation published by Atomizdat, Moscow (1967)].
[87]A. Bohr and B. Mottelson, Nuclear Structure, Vol. 1, Benjamin, Reading, Mass. (1975) [Russian translation published by Mir, Moscow (1977), p. 295].
[88]B. B. Back, Nucl. Phys. **A228**, 323 (1974).
[89]Yu. B. Ostapenko, Vopr. At. Nauki Tekh., Ser. Yad. Konst. **36**, 12 (1980).
[90]S. B. Ermagambetov, V. E. Kolesov, V. G. Nesterov, *et al.*, Yad. Fiz. **8**, 704 (1968) [Sov. J. Nucl. Phys. **8**, 409 (1969)].
[91]A. V. Ignatyuk, K. K. Istekov, and G. N Smirenkin, Yad. Fiz. **29**, 875 (1979) [Sov. J. Nucl. Phys. **29**, 450 (1979)].
[92]J. E. Lynn, UKAEA Report AERE-R7468, Harwell (1974).
[93]P. A. Russo, J. Pedersen, and R. Vandenbosch, in: Proc. Intern. Conf. on the Physics and Chemistry of Fission, Vol. 1, IAEA, Vienna (1974), p. 271.
[94]W. Günther, K. Huber, U. Kneissl, *et al.*, Nucl. Phys. **A297**, 254 (1978).
[95]B. S. Dzhelepov, L. K. Peker, and V. O. Sergeev, Skhemy raspada radioaktivnykh yader (Decay Schemes of Radioactive Nuclei), USSR Academy of Sciences, Moscow-Leningrad (1963).
[96]G. V. Anikin, V. I. Popov, and I. I. Kotukhov, Preprint No. 405 [in Russian], Physics and Power Institute, Obninsk (1973).
[97]S. E. Larsson and G. Leander, in: Ref. 93, p. 177.
[98]B. S. Bhandari, Phys. Rev. C **19**, 1820 (1979).
[99]B. S. Bhandari, Phys. Rev. C **22**, 606 (1980).
[100]Yu. B. Ostapenko, G. N. Smirenkin, A. S. Soldatov, *et al.*, in: Ref. 70, p. 78.
[101]M. Asghar, Z. Phys. **A286**, 299 (1978).
[102]M. Brack, J. Damgaard, H. C. Pauli, *et al.*, Rev. Mod. Phys. **44**, 320 (1972).
[103]Yu. A. Selitskiĭ, Fiz. Elem. Chastits At. Yadra **10**, 314 (1979) [Sov. J. Part. Nucl. **10**, 121 (1979)].

Translated by Julian B. Barbour